IONIC CHARGE DETERMINATION

BY ION-EXCHANGE TECHNIQUES

IONIC CHARGE DETERMINATION BY ION-EXCHANGE TECHNIQUES

A thesis submitted in partial fulfilment of the requirements for admission to the degree of Master of Science of the University of Sydney.

by

DARRYL W. YANIUK

March 1972

Department of Inorganic Chemistry

University of Sydney

TABLE OF CONTENTS

Summary

The experimental limitations of the "inverse batch equilibrium" method of charge determination have been delineated and the technique has been successfully applied to simple, complex and polymeric ions.

SECTION 1

INTRODUCTION

1.1 A Review of Charge Determination by Ion-Exchange

The competition between two ions for exchange sites on an ion-exchange resin can be measured and used to determine the charge carried by a simple or complex ion in solution.

Strickland[1] was the first to introduce this competative effect into an equation for the calculation of ionic charge. His method was based on the batchwise equilibration of two ions, one of known charge, the other of unknown charge, with an ion-exchange resin in the presence of a supporting electrolyte. Variation of the concentration of the ion of known charge was used to change the distribution of the ions between the aqueous and the resin phase. A plot of the logarithm of the concentration of the ion of known charge versus the logarithm of the distribution coefficient of the ion of unknown charge resulted in a straight line. The unknown charge could then be calculated from the ratio of the slope of this line to the known charge.

Strickland's method has been used by several authors and, in conjunction with other evidence, has provided positive identification of many complex ions.

In 1952 Welch[2] applied the method in his study of the protactinate ion in perchloric acid solutions (0.1 to 0.3 M). He obtained a value of plus one for the charge of this ion and assumed its formula to be PaO_2^+.

In 1958 Cady and Connick[3] determined the charges of several chloro complexes of ruthenium in perchloric acid solutions. These indicated the presence of the complex ions Ru^{3+}, $RuCl^{2+}$ and $RuCl_2^+$.

The following year Jakovac and Lederer[4] investigated the charge of the protactinate ion in alkaline solution. They found the ion to have a negative charge of three, identical to that of the phosphate ion determined under similar conditions.

B.I.Nabivanets[5] used the method on titanium (IV) in aqueous perchloric acid solutions and charges of plus one and plus two were calculated. These were assigned to the ions $TiO(OH)^{+}$ and TiO^{2+} respectively.

A study of the charges of ions formed in beryllium solutions led Curley[6] to postulate the existence of a tripositive ion at pH values above 4.5. This corroborated the work of Kakihana and Sillen[7] who had proposed that $Be_3(OH)_3^{3+}$ was the predominant species in beryllium solutions at pH values greater than 3.5.

Smith[8] was able to show that niobate and tantalate ions carried a negative charge of seven in alkaline solution and proposed the formulas $HNb_6O_{19}^{7-}$ and $HTa_6O_{19}^{7-}$ for these ions.

Evidence for the existence of the bipositive mercury(I) ion (Hg_2^{2+}) was provided by Cooper and Foster[9]. They measured changes in the distribution of mercury(I) between the solution and resin phases with variations in the hydrogen ion concentration of nitric acid solutions.

In 1959 Trofimov and Stepanova[10] developed another method whereby ionic charges could be calculated. This method,in contrast to that of Strickland, was based upon the variation of the distribution of the ion of unknown charge

with changes in resin volume.

Solutions of the ion of unknown charge, in the presence of a supporting electrolyte, were equilibrated with two resins having different specific volumes. The logarithm of the ratio of the distribution coefficients measured for each resin sample, together with the logarithm of the ratio of the specific volumes of the two resins, ~~were~~ was used to calculate the apparent charge of the ion in solution.

The same authors[10a] have used this method to determine the charges of nitrato complexes of zirconium. These complexes were found to vary in composition with nitric acid concentration, the variations being ascribed to complexing and polymerisation reactions.

Grinberg, Trofimov and Stepanova[11] determined the apparent charge of polynuclear ruthenium complexes in sodium nitrate solutions. They have reported a charge of six for the red nitrato complex of ruthenium.

An investigation[12] of the charge carried by the oxalato complex of uranium gave a value of four, which was ascribed to the ion $U(C_2O_4)_4^{4-}$. Further studies[13] of the oxalato complexes of several actinide elements, namely thorium, uranium and neptunium, gave values which could be assigned to complexes with charges of zero, -1, -2, and -4, depending upon the oxalate concentration of the solution.

R.M.Wallace[14] has developed a novel method for charge determination based upon the Donnan equilibrium across ion-exchange membranes. This was successfully applied to the

determination of the charges carried by a number of simple ions in solution.

A columnar method, based on the plate theory of Mayer and Tompkins[15] was used by Garman[16] in another effort to establish the identity of the predominant ion in beryllium solutions at pH 5.5. Detection of an ion with a charge of +3 provided evidence for the existence of the ion $Be_3(OH)_3^{3+}$ proposed by other workers.

1.2 Polymeric Ions

The methods outlined above have been successful in their application to simple and complex mononuclear ions but the experimental conditions prevent their use for the determination of the charges of polymeric species such as those formed by the condensation of several monomeric units. These exist usually at relatively high solution concentrations.

In each of the experiments discussed in the literature, the solution phase consisted of low concentrations($< 10^{-3}$ M) of the ion of known charge, and a supporting electrolyte.

For the unequivocal assignment of a charge value to a polymeric ion it must be the predominant ionic species in solution. The presence of other counter-ions in appreciable concentrations changes the distribution of the known ion between the two phases and leads to inaccuracies in the determinations. Since a supporting electrolyte contains a high concentration of a counter-ion other than the one under investigation it can not be used in this situation.

1.3 Scope of the Present Work

To overcome the problems referred to above (section 1.2) a new method of charge determination has been developed. It is based on the method of Strickland[1] but is modified in that the ion of known charge is present at trace levels (approximately 10^{-10} M). There is no supporting electrolyte, and the polymeric ion whose charge is to be determined occurs at relatively high concentrations ($> 10^{-3}$ M). This method has been called "the inverse batch equilibrium method of charge determination", since the concentrations of the competing ions are reversed in comparison to previous methods.

As a preliminary test of the inverse batch equilibrium method model systems were formulated for both anions and cations. Each system was set up with a simple monomeric ion of known charge as the "unknown" and the apparent charges of these ions were measured then compared with their commonly accepted values.

The experimental restrictions for the model systems were based on those of Kraus and Nelson[17]. Intentional deviations from these restrictions were investigated with the view to finding the ideal conditions for charge determination.

After this preliminary work the method was applied to the determination of the charge of a complex ion (the tris(ethylenediamine)nickel(II) cation), and two polymeric ions, the dichromate ion whose charge has been well established, as well as the previously mentioned hydrolysis

polymer formed in slightly acidic beryllium solutions. The nature of the latter ion has been the centre of much controversy and it seemed that this new method of charge determination might well lead to an unambiguous formula.

1.4 Previous Work on the Hydrolysis of Beryllium in Acidic Solutions

The extent of polymerisation of the simple beryllium ion in acidic solution has been disputed for many years. A review[16] of the work carried out up to 1968 shows the numerous species that have been suggested. Most commonly accepted are those proposed by Kakihana and Sillen[7]. These include the trimer $Be_3(OH)_3^{3+}$, the ion $(Be_2OH)^{3+}$, and the simple Be^{2+} ion. The trimer was thought to predominate in moderately concentrated beryllium solutions (circa 50 mM) in the pH range 4.8 to 6.0.

Investigations[18,19,20] since 1968 have tended to confirm the existence of the above three ions. In addition evidence has been provided for the presence of several new ionic species. Carpeni and Lanza[21] showed by pH-titration that in addition to the three ions already mentioned, the ions $Be_3(OH)_4^{2+}$, $Be_6(OH)_8^{4+}$, and $Be_6(OH)_9^{3+}$ were present in aqueous solutions of beryllium nitrate containing potassium nitrate (2 M) as the supporting electrolyte. These results were supported by Lanza[22] working with beryllium chloride in potassium chloride (2 M) and with beryllium sulphate in potassium sulphate (0.1 M) solutions.

SECTION 2

THEORY

2.1 The Inverse Batch Equilibrium Method of Charge Determination

2.1.1 The system

If the charge on an ion, A^z, is to be determined by the inverse batch equilibrium method of charge determination, the following requirements must be met.

(i) The ion-exchange resin must be pre-treated so that the ion A^z occupies all the exchange sites.

(ii) The solution phase, in equilibrium with the resin, must contain macro concentrations of the ion A^z.

(iii) An ion of known charge, B^x, must be present in the solution at micro concentrations.

An equilibrium system is set up so that the ion B^x competes with the ion A^z for exchange sites on the resin. Measurement of the extent of this competition leads to the calculation of a value for the apparent charge carried by the ion A^z in solution.

2.1.2 Derivation of the relevant equation

When an ion-exchange resin, containing ions of the form A^z, is in contact with a solution containing the ion A^z and another counter-ion B^x, the following equilibrium is set up.

$$zB^x + x\bar{A}^z \rightleftharpoons z\bar{B}^x + xA^z \qquad \ldots(1)$$

Barred symbols represent the resin-phase species.

Provided that electrolyte sorption and changes in swelling of the resin are small, a thermodynamic equilibrium constant[23a] may be written for equation (1).

$$K = \frac{(a_{\bar{B}})^z (a_A)^x}{(a_B)^z (a_{\bar{A}})^x} \quad \ldots.(2)$$

$$= \frac{(C_{\bar{B}})^z (C_A)^x}{(C_B)^z (C_{\bar{A}})^x} \cdot \frac{(\gamma_{\bar{B}})^z (\gamma_A)^x}{(\gamma_B)^z (\gamma_{\bar{A}})^x} \quad \ldots.(3)$$

Where a_A, $a_{\bar{A}}$, a_B, $a_{\bar{B}}$, C_A, $C_{\bar{A}}$, C_B, $C_{\bar{B}}$, γ_A, $\gamma_{\bar{A}}$, γ_B, and $\gamma_{\bar{B}}$ represent the activities, concentrations and activity coefficients of the ions A^z, $\bar{A}^z$, B^x, and $\bar{B}^x$ respectively.

Re-arranging equation (3),

$$K = \left(\frac{C_{\bar{B}}}{C_B}\right)^z \cdot \frac{(C_A)^x (\gamma_A)^x}{(C_{\bar{A}})^x} \cdot \frac{(\gamma_{\bar{B}})^z}{(\gamma_B)^z (\gamma_{\bar{A}})^x} \quad \ldots.(4)$$

The distribution coefficient, D_B, for the distribution of the ion B^x between the two phases has been defined[23b] as,

$$D_B = \frac{C_{\bar{B}}}{C_B} \quad \ldots.(5)$$

Substituting for D_B into equation (4),

$$K = (D_B)^z \cdot \frac{(a_A)^x}{(C_{\bar{A}})^x} \cdot \frac{(\gamma_{\bar{B}})^z}{(\gamma_B)^z (\gamma_{\bar{A}})^x} \quad \ldots.(6)$$

Re-arranging equation (6),

$$D_B = K^{1/z} . (C_{\bar{A}})^{x/z} . (a_A)^{-x/z} . (\gamma_{\bar{B}})^{-1} . (\gamma_B) . (\gamma_{\bar{A}})^{x/z} \quad \ldots.(7)$$

Taking logarithms of both sides of equation (7),

$$\log D_B = \frac{1}{z}.\log K + \frac{x}{z}.\log C_{\bar{A}} - \frac{x}{z}.\log a_A - \log \gamma_{\bar{B}} + \log \gamma_B + \frac{x}{z}.\log \gamma_{\bar{A}} \quad \ldots.(8)$$

Differentiating equation (8) with respect to $\log a_A$,

$$\frac{\partial \log D_B}{\partial \log a_A} = -\frac{x}{z} + \frac{x}{z}.\frac{\partial \log C_{\bar{A}}}{\partial \log a_A} + \frac{\partial \log \gamma_B}{\partial \log a_A} + \frac{\partial \log (\gamma_{\bar{A}}^{x/z}/\gamma_{\bar{B}})}{\partial \log a_A} \quad \ldots.(9)$$

Under certain limiting conditions[17] this may be simplified to,

$$\frac{\partial \log D_B}{\partial \log a_A} = -\frac{x}{z} \quad \ldots.(10)$$

That is,

$$\frac{x}{z}.\frac{\partial \log C_{\bar{A}}}{\partial \log a_A} + \frac{\partial \log \gamma_B}{\partial \log a_A} + \frac{\partial \log (\gamma_{\bar{A}}^{x/z}/\gamma_{\bar{B}})}{\partial \log a_A} \xrightarrow{\text{limit}} 0 \quad \ldots.(11)$$

Integrating equation (10) with respect to $\log a_A$,

$$\log D_B = -\frac{x}{z}.\log a_A + \text{constant} \quad \ldots.(12)$$

Whitney and Diamond[24], working over a wide range of solution concentrations (10^{-1} to 10 M), showed that the activity term of equation(12) could be replaced by a concentration term without seriously affecting their results. The equation can then be expressed in the following form.

$$\log D_B = -\frac{x}{z}.\log C_A + \text{constant} \quad \ldots.(13)$$

The use of equation (13) is governed by the conditions set out in equation (11). If these conditions are obeyed a double logarithm plot of the distribution coefficient of the ion B^x against the concentration of the ion A^z gives a straight line. The slope of the line is related to the ratio of the charges of the ions B^x and A^z.

$$\text{slope} = -\frac{x}{z} \quad \ldots.(14)$$

As the charge of the ion B^x is known the apparent charge, z, carried by the ion A^z in solution may be calculated with equation (14).

Equation (11) becomes valid only if the following restrictions[17,23c] are imposed.

(a) The concentration of A^z should be very much greater than the concentration of the ion B^x.

(b) Variations in the concentration of A^z should be small.

(c) The charge of the ions A^z and B^x should not alter under the experimental conditions.

The application of condition (a) indicates that uptake of B^x by the resin will be small, that is $C_{\bar{A}} >> C_{\bar{B}}$. This, together with condition (b), implies that the change in $C_{\bar{A}}$ with changes in the concentration of A^z will be very small.

That is, $\frac{\partial \log C_{\bar{A}}}{\partial \log a_A}$ is approximately zero in equation (11).

Furthermore, while the change in the macrocomponent concentration (C_A) is small the ratio of the activity coefficients of the two ions in the resin phase will be approximately constant so that,

$\frac{\partial \log (\gamma_{\bar{A}}^{x/z} / \gamma_{\bar{B}})}{\partial \log a_A}$ is approximately zero in equation (11).

The overall electrolyte concentration is large when compared to that of the trace ion, B^x. As a result of this the activity coefficient of B^x remains relatively constant and,

$\frac{\partial \log \gamma_B}{\partial \log a_A}$ is approximately zero in equation (11).

Under the conditions set out above, equation (10) becomes valid and equations (13) and (14) are suitable for the calculation of the charge of an ion in solution.

2.2 Choice of Ion-Exchange Resins for the Model Systems

As stated previously (section 2.1.2) electrolyte sorption by the resin and changes in the swelling of the resin must be small to make equations (13) and (14) valid.

Electrolyte penetration into the resin matrix is controlled by the Donnan[25,26] potential. The efficiency of this control is increased[23d] with resins of high capacity and a high degree of crosslinkage.

The tendency of a resin to swell is favoured[23e] by a low degree of crosslinkage, high capacity and strong solvation of the fixed ionic groups.

In order that the requirements for electrolyte sorption and resin swelling be met it is necessary to employ a resin which has a moderately high degree of crosslinkage together with a large capacity for exchange. The mesh size of the resin should not be important as it is only a measure of the size of the resin beads.

2.3 The Effect of Deviations from the Restrictions Imposed on the Model Systems

Departure from the restrictions imposed in the derivation of equation (13) should lead to alterations in the slope of the double logarithm plot obtained from this

equation. In most cases these deviations can be explained as infringements of equation (11).

2.3.1 Macro-ion to micro-ion concentration ratio

The ratio of the concentration of the macrocomponent (A^z) to the concentration of the microcomponent (B^x) should be very large. It has been suggested[27,28,29] that a ratio of greater than 10^4 to 1 must be employed. A decrease in this ratio causes the microcomponent to compete more strongly for exchange sites on the resin thereby invalidating the assumptions made in equation (11).

As a result of this increased competition changes in the concentration of A^z on the resin will be significant and the first term of equation (11), $\frac{\partial \log C_{\bar{A}}}{\partial \log a_A}$, will not approximate zero. Equation (10) will be modified by inclusion of this term and the graph obtained from equation (13) will be non-linear. This curvature would bring about a decrease in the slope of the straight line of best fit calculated by least squares analysis (Appendix 2) and a resulting increase in the apparent charge.

2.3.2 Variation of the concentration of the ion A^z

Large variations in the concentration of the macrocomponent ion (A^z) bring about changes in the ratio of the resin phase activity coefficients of the ions A^z and B^x. This, in turn, invalidates the assumption that the term

$\frac{\partial \log (\gamma_{\bar{A}}^{x/z}/\gamma_{\bar{B}})}{\partial \log a_A}$ approximates zero.

In addition a large change in the concentration of A^z causes the equivalent volume of the resin to vary. Changes in resin swelling, as measured by the equivalent volume, affect electrolyte penetration into the resin matrix thereby violating the assumption that the terms

$\frac{\partial \log C_{\bar{A}}}{\partial \log a_A}$ and $\frac{\partial \log (\gamma_{\bar{A}}^{x/z}/\gamma_{\bar{B}})}{\partial \log a_A}$ are effectively zero.

These infringements on the conditions governing the successful application of equation (13) should again be noticeable in a curving of the double logarithm plot of distribution coefficient versus the concentration of A^z and an apparent increase of charge. The effect should be most prominent in resins with a low degree of crosslinkage as these are most susceptible to variations in equivalent volume.

2.3.3 The competing ions

An important factor in charge determination by the inverse batch equilibrium method is the choice of competing ions. A basic condition which must be obeyed in this method is that the charge on the ions involved must not change during the course of the experiment.

In general the ion of unknown charge is present in a solution which has no effect on its charge. The competing microcomponent ion of known charge must be chosen so that the charge is not altered by any of the ions which are

present at macroconcentrations. It can be seen from the equation (14) used to calculate the charge from the slope of a straight line that a variation in the charge of the microcomponent ion of known charge would alter the calculated value of the ion under investigation.

2.3.4 Effect of the exchange capacity of the ion-exchange resins

The capacity of a resin for counter-ions may also be significant in charge determinations. It has already been noted (section 2.2) that a high capacity for exchange is desirable to control the extent of electrolyte penetration into the resin matrix. If this capacity is exceptionally low there will be a drop in the Donnan potential which will allow significant migration of A^z into the resin phase. This migration will vary with the concentration of A^z and thus the assumption that $\frac{\partial \log C_{\bar{A}}}{\partial \log a_A}$ is approximately zero will be invalid.

2.4 Investigations

Each of the points discussed above were investigated. In the first instance model systems were set up to determine the charges on simple anions and cations. For these determinations all the restrictions which were imposed for the development of equation (13) were applied. By removing the restrictions, one at a time, their effect on the calculated charge of the macrocomponent ion (A^z) was evaluated.

SECTION 3

EXPERIMENTAL

3.1 Materials

Chemicals

All chemicals, with the exception of naphthalene, sodium iodide, and magnesium perchlorate, were analytical grade. Reagent grade naphthalene was recrystallized from ethanol (absolute) before use. Sodium iodide and magnesium perchlorate were recrystallized from water.

Water

Distilled water was used for the preparation of solutions and the washing of ion-exchange resins.

Magnesium perchlorate solutions

Recrystallized magnesium perchlorate was dissolved in water and the resulting solutions analysed for magnesium with EDTA and eriochrome black T[30a].

Beryllium perchlorate solutions

Stock solutions of beryllium perchlorate were prepared by reacting beryllium powder with an excess of perchloric acid. The solutions to be used for distribution measurements were prepared by appropriate dilution of the stock solutions. These solutions were adjusted to the required pH with hydroxide form anion-exchange resin thus avoiding the addition of another cation. Analysis for beryllium was carried out spectrophotometrically[31] with chrome azurol S.

Buffers

The pH meter was standardised with Radiometer buffer solution and Burroughs Wellcome buffer tablets which when prepared as directed gave solutions of pH 6.48 and 3.97

respectively at 20°.

Standard solutions

Solutions of silver nitrate (0.100 M), hydrochloric acid (0.100 M), and sodium hydroxide (0.100 M) were prepared as directed from BDH concentrated volumetric solutions. The hydrochloric acid was used as a third standard for the pH meter. It has a pH[30b] of 1.10 at 20°.

Tris(ethylenediamine)nickel(II) chloride solutions

Tris(ethylenediamine)nickel(II) chloride dihydrate was prepared[32] from nickel(II) chloride hexahydrate and ethylenediamine. It was recrystallized from water and a stock solution prepared by dissolving the recrystallized compound in water. This solution was analysed for nickel by atomic absorption spectroscopy[33]. Dilutions of the stock solution were used for the distribution measurements.

Sodium iodide solutions

These were prepared by dissolving recrystallized sodium iodide in water. The iodide ion concentration was determined by Volhard's method[30c].

Sodium and potassium chloride solutions

These were prepared from analytical grade sodium and potassium chloride by direct weighing of the solid followed by dilution to the appropriate volume.

Radioisotopes

All radioisotopes were obtained from the Radiochemical Centre, Amersham, Buckinghamshire, England. They were supplied to the following specifications.

Sodium-22:- as sodium chloride in aqueous solution.
Specific activity approximately 60 mCi/mg Na.

Sulphur-35:- as carrier free sodium sulphate in aqueous solution.

Calcium-45:- as calcium chloride in aqueous solution.
Specific activity 50mCi/mg Ca.

Cobalt-60:- as potassium hexacyanocobaltate(III) in aqueous solution. Specific activity approximately 1 mCi/mg Co.

Caesium-137:- as caesium chloride in hydrochloric acid (1 M).

Cerium-144:- as cerium(III) chloride in hydrochloric acid (1 M).

Liquid scintillation solutions

A dioxane based liquid scintillation solution[34] was used for the measurement of the β-radiation produced by sulphur-35 and calcium-45. Each litre of solution contained naphthalene (50g), 2,5-diphenyloxazole (6g) and 1,4-bis-2-(5-phenyloxazolyl)-benzene (0.1g).

For the counting of the radiation produced by sulphur-35 in the presence of iodide ions the liquid scintillation solution was modified by the addition of acetone (500ml/litre of dioxane). This modification was introduced to remove free iodine from the scintillation solution as it combined with the dioxane to form complexes[35] which, being yellow in colour, absorbed light of the wavelength seen by the photomultiplier tube and consequently lowered the counting efficiency.

Ion-exchange resins

The following ion-exchange resins were used.

Cation-exchange resins.

Dowex 50W; X1; X4; X8, 50-100 mesh.

Zeo-Karb (SRC 15), 8% divinylbenzene, 100-200 mesh.

Amberlite CG 120, 8% divinylbenzene, 100-200 mesh.

Anion-exchange resins.

Dowex 1X8, 50-100, 100-200 and 200-400 mesh.

Dowex 1X1, 50-100 mesh.

De-Acidite FF(IP), (SRA 71), 7-9% average divinylbenzene, 100-200 mesh.

De-Acidite FF, (SRA 63), 2-3% average divinylbenzene, 100-200 mesh.

Amberlite IRA-400, 3-5% average divinylbenzene, 100-200 mesh.

Dowex 21K, 30-50 and 50-100 mesh.

Before use each of the resins was conditioned by a standard method[23f]. This involved thorough washing of each resin followed by the decanting of fines. The resin was then loaded into a column where it was alternately treated with solutions of sodium hydroxide (1 M) and hydrochloric acid (1 M). Between acid and alkali the resin was washed with water until neutral to BDH indicator paper. After conditioning, the resin was stored under water until required.

Anion-exchange resins, Dowex 1X8 and Dowex 21K, which had been used for adjusting the pH of beryllium perchlorate solutions were in the perchlorate form and were regenerated by washing with sodium dichromate solution, followed by iron(II) ammonium sulphate in hydrochloric acid solution (4 M). The iron(III) produced by the reaction between chromium(VI)

and iron(II) was present on the resin as the tetrachloroferrate(III) ion. It was removed by passing dilute hydrochloric acid (0.05 M) through the resin. The resin was then converted to the hydroxide form with excess sodium hydroxide solution (1 M). This complex method of regeneration was necessary because of the exceptionally high affinity of the perchlorate ion for the resin.

3.2 Apparatus

Balance

Quantitative weighings were made on a Mettler M6 analytical balance with an accuracy of $\pm$ 2 x 10^{-4}g.

pH meter

The pH of aqueous solutions was measured with a Radiometer model PHM4C meter[36]. A glass electrode, type G200B, was used in conjunction with a modified calomel electrode, type K100. The calomel electrode was modified to prevent precipitation of potassium perchlorate when measuring the pH of beryllium perchlorate solutions. The modification was achieved by joining the liquid junction of the electrode to a capillary tube containing Whatman accelerator paper and saturated potassium chloride solution.

Batch equilibrium apparatus

The equilibration of ion-exchange resins with labelled solutions was carried out in polystyrene pill packs (30ml capacity) which were made watertight by binding a strip of Parafilm around the neck of the pill pack before replacing the lid. For solution volumes greater than 30ml,

polythene bottles with screw-on tops were used. Glass containers could not be used owing to the tendency of glass to absorb radioisotopes.

Radioactive counting equipment

Gamma radiation

The quantitative measurement of the γ-radioactivity produced by the radioisotopes sodium-22, cobalt-60, caesium-137, and cerium-144 was made with a Philips single-channel gamma-ray spectrometer, set to measure integral count rates.

To determine the working voltage of the detector the energy spectrum of each radioisotope was scanned over a range of EHT values of the photomultiplier tube. Typical spectra are shown in Figure 1. The plateau regions indicate suitable working voltages. Table 1 lists the EHT values chosen for each isotope.

TABLE 1

Conditions for the measurement of γ-radiation

Isotope	EHT(volts)	Attenuation	Lower Level
sodium-22	1050	2	0.50
cobalt-60	950	2	0.50
caesium-137	950	3	0.70
cerium-144	1050	4	0.70

Beta radiation

Modification of the circuitry of the single-channel gamma spectrometer to include a coincidence unit, a second EHT supply, and a scintillation detector enabled the

Figure 1

Energy Spectra of the γ-Emitting Radioisotopes.

Sodium-22

Cobalt-60

Caesium-137

Cerium-144

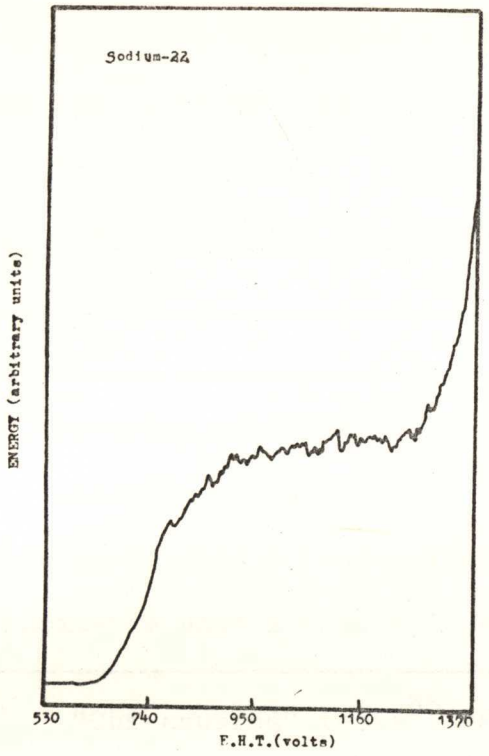
Sodium-22
ENERGY (arbitrary units)
530
740
950
1160
1370
E.H.T.(volts)

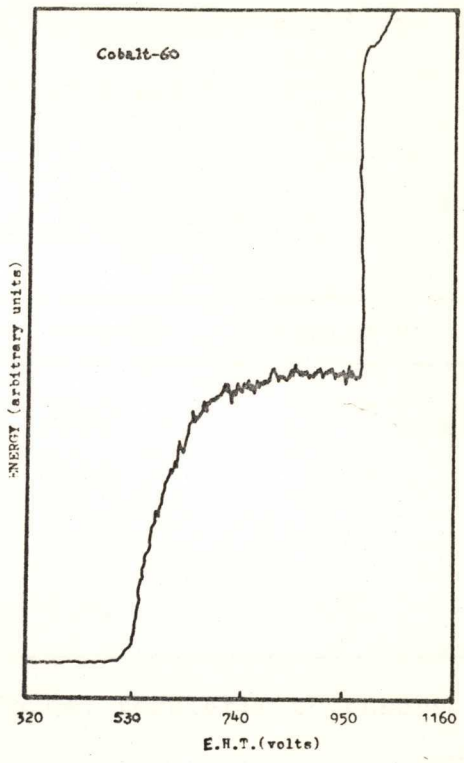
Cobalt-60
ENERGY (arbitrary units)
320
530
740
950
1160
E.H.T.(volts)

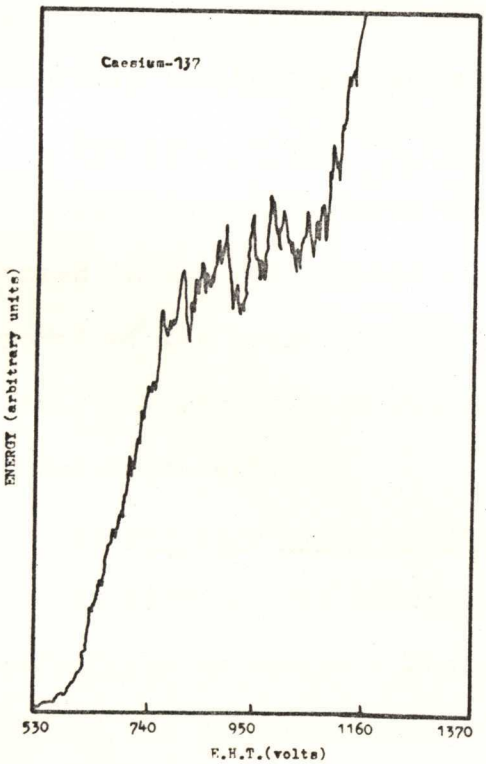
Caesium-137
ENERGY (arbitrary units)
530
740
950
1160
1370
E.H.T.(volts)

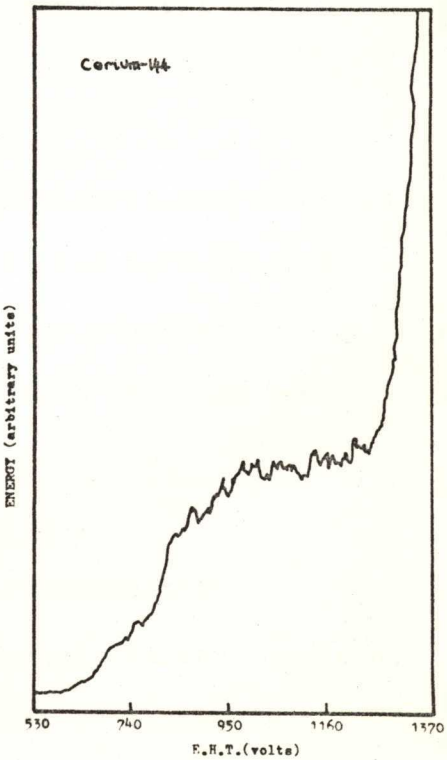
Cerium-144
ENERGY (arbitrary units)
530
740
950
1160
1370
E.H.T.(volts)

quantitative counting of the β-radiation produced by the radioisotopes sulphur-35 and calcium-45. Counting conditions were chosen by the method outlined in the appropriate Philips handbook[37]. These conditions are given in Table 2.

TABLE 2

Conditions for the measurement of β-radiation

	sulphur-35	calcium-45
Detector A (volts)	1760	1660
Detector B (volts)	1710	1610
Coincidence unit A (lower level)	0.40	0.60
Coincidence unit B (lower level)	0.40	0.60

"Chi-squared" tests[38] were performed regularly to ensure that the spectrometer was not counting spurious pulses. The calculated values of "chi-squared" always fell within acceptable limits[39] for accurate counting.

Counting phials

Solutions containing the gamma-emitting isotopes were counted in 5ml polystyrene vials that fitted into the well crystal of the scintillation detector. The counting of β-radiation was carried out in silica glass vials of low potassium content.

Atomic absorption spectrophotometer

An A1750 atomic absorption spectrophotometer, manufactured by Southern Analytical Limited, Surrey, England, was used for the quantitative measurement of nickel in the tris(ethylenediamine)nickel(II) complex ion.

Centrifuge

Samples of ion-exchange resin used in the calculation of equivalent volumes were centrifuged with a "Tosco MSE" centrifuge manufactured by Thomas Optical Company Pty. Ltd., Sydney, Australia.

3.3 Experimental Methods

3.3.1 Batch equilibrium experiments

Preparation of the resin

In order to carry out distribution measurements by batch equilibration experiments it was necessary to convert the resin into the form of the ion whose charge was to be determined. This was achieved by passing a solution of the ion through a column of the resin until the influent and effluent solution concentrations were the same. The exchanger was then washed with water and stored under water until required.

Beryllium form cation-exchange resin

Preparation of this resin was slightly different from that of the other resins in that the extent of conversion to the beryllium form was measured by recording the pH of the influent and effluent solutions. Conversion was deemed to be complete when both these values agreed to within $\pm$ 0.02 of a pH unit.

Since the beryllium species in the resin phase was a hydrolysis polymer the resin could not be washed with water after it had been converted to the appropriate form. It was therefore stored in contact with the solution with

which it had been equilibrated.

Preparation of the solution phase

For each charge determination experiment a series of solutions was prepared. These solutions contained a known concentration of the species under investigation and an appropriate radioisotope. There was no supporting electrolyte in any solution.

Distribution experiments

Ion-exchange resin which had been converted to the required form and stored under solution was sucked dry at the pump for twenty minutes. To determine the moisture content, and hence the dry weight, of the resin duplicate samples were taken and heated to constant weight in an oven at 65°. A suitable amount of resin was weighed into each equilibration vessel and a predetermined volume of isotopically labelled solution added.

Contact between the two phases was maintained for seven days for simple systems and for greater than fourteen days in the case of complex and polymeric ions. It has been established[40] that equilibrium is usually achieved before this time.

After equilibration the resin was allowed to settle and the solution phase decanted. Duplicate samples of the solution were taken and, together with the samples taken before equilibration, were analysed by radioactive counting.

Distribution coefficients were calculated from these measurements by the method given in Appendix 1. The charge

on the unknown ion was determined by the method of least squares as described in Appendix 2.

3.3.2 Determination of the capacities of ion-exchange resins

Anion-exchange resins

The capacity of each of the anion-exchange resins was determined by measuring the chloride ion content of a known amount of dry resin[41a]. The chloride form resin was sucked dry at the pump and three samples were weighed out and transferred quantitatively to semi-micro columns. Samples were also weighed for the determination of the moisture content of each resin.

A solution of sodium nitrate (0.25 M) was run through each column. As strongly basic anion-exchange resins have a greater affinity[42] for nitrate ions than chloride ions, the latter was eluted from the column and collected in volumetric flasks (250ml). The solutions were diluted to the mark and aliquots (50ml) were taken for chloride analysis with silver nitrate (0.100 M) using potassium chromate indicator[30d] (Mohr method). The capacity of each resin, expressed in milliequivalents of chloride ion per gramme of dry resin, is recorded in Appendix 3.

Cation-exchange resins

Three weighed samples of strongly acidic cation-exchange resin, in the hydrogen form, were transferred to semi-micro columns where the hydrogen ions were eluted by passing potassium chloride (0.5 M) through the columns[41b].

The eluate was collected in volumetric flasks (250ml), diluted to the mark and samples (50ml) taken for analysis with sodium hydroxide (0.100 M) using phenophthalein indicator[30e]. The capacities of each cation-exchange resin, expressed in milliequivalents of hydrogen ion per gramme of dry resin, are also recorded in Appendix 3.

3.3.3 Measurement of the swelling of ion-exchange resins

To determine the changes in swelling of the resins under different solution conditions four samples of each chloride form anion-exchange resin and potassium form cation-exchange resin were weighed into graduated centrifuge tubes. Various concentrations of solutions of sodium chloride (for anion-exchange resins) and potassium chloride (for cation-exchange resins) were added to each tube. The tubes, and their contents, were centrifuged for 15 minutes at 2000 r.p.m. This was repeated until the volume of resin remaining at the end of centrifugation was constant. The values obtained were used to calculate the equivalent volume[23h] of the resin at each solution concentration. The results are given in Appendix 4.

3.4 Errors

As a result of the inaccuracies introduced in the physical measurement of the distribution coefficients a limit of accuracy of 5% was set on the value of the determined charge. A charge within 5% of the known charge was deemed to be correct while those outside this range were incorrect and were usually the result of an infringement of the restrictions placed upon the method (section 2.1.2).

SECTION 4

RESULTS AND DISCUSSION

4.1 Batch Equilibrium Experiments

4.1.1 Model systems

The term "model" is used to represent an experimental system in which all the restrictions outlined in the theory (section 2.1.2) have been applied. It is expected that charges calculated with these systems will be accurate and will correspond to the known value of the charge of the ion under investigation.

The simple ions which were used as the "unknowns" in the model systems were the chloride and potassium ions. These were the macrocomponent counter-ions in the solution phase of the batch equilibrium experiments.

For anionic systems sulphate ion, labelled with sulphur-35, was the microcomponent and the anion-exchange resins were in the chloride form. In the cationic systems trace concentrations of sodium-22 labelled sodium ion ($^{22}Na^{+}$) were used. The cation-exchange resins contained potassium ions as the counter-ions.

Radioactive counting of the solutions before and after equilibrium had been attained enabled calculation of the distribution coefficients recorded in Appendices 5 and 6. A summary of the experimental conditions, and the measured charges, is given in Table 3.

TABLE 3

Measurement of the charges of potassium and chloride ions

(model systems)

In this and all succeeding tables "divinylbenzene" is abbreviated to "DVB".

Macrocomponent concentration range.

Chloride ion (as NaCl): 7.14×10^{-1} to 1.67×10^{-2} M.

Potassium ion (as KCl): 4.00×10^{-1} to 4.00×10^{-3} M.

Microcomponent concentration.

Sulphate ion (as $Na_2{}^{35}SO_4$): $\sim 10^{-10}$ M.

Sodium ion (as $^{22}NaCl$): $\sim 10^{-10}$ M.

Resin	Apparent charge	Appendix and figure
Chloride ion (sulphate ion as microcomponent)		
Dowex 1X8	-0.96 ± 0.02	5, 5a
De-Acidite FF(IP) 7-9% DVB	-1.03 ± 0.03	5, 5b
Amberlite IRA-400 3-5% DVB	-0.99 ± 0.04	5, 5c
Potassium ion (sodium ion as microcomponent)		
Dowex 50WX8	$+1.03 \pm 0.02$	6, 6a
Zeo-Karb (SRC15) 8% DVB	$+1.01 \pm 0.03$	6, 6b
Amberlite CG-120 8% DVB	$+1.01 \pm 0.04$	6, 6c

The values of minus one and plus one obtained for the charges of the chloride and potassium ions agree respectively, within the limits of experimental error (section 3.4), with the accepted charges of these ions.

4.1.2 Variation of the resin mesh size

There was no reference to the size of the resin beads in the restrictions (section 2.1.2) imposed on the inverse batch equilibrium method of charge determination as it was not expected that this would be an important factor with this technique.

Nevertheless an investigation into the possible effect of the bead size was carried out with three chloride form anion-exchange resins having 8% divinylbenzene and with U.S. mesh sizes 50-100, 100-200 and 200-400. The solutions in equilibrium with each resin were composed of high concentrations of chloride ions with sulphate ion as the microcomponent.

Table 4 contains the results of these determinations. charges of minus one were calculated for the chloride ion in each case except for the experiment with 200-400 mesh resin (-0.93 $\pm$ 0.02). The cause of the inaccuracy here is unknown.

TABLE 4

The charge of the chloride ion with resins of differing mesh size

Anion-exchange resin:- Dowex 1X8.

Microcomponent concentration.

Sulphate ion (as $Na_2{}^{35}SO_4$): $\sim 10^{-10}$ M.

Mesh size	Chloride ion concentration range (moles/litre)	Apparent charge	Appendix and figure
50-100	7.14×10^{-1} to 1.67×10^{-2}	-0.96±0.02	7,7a
100-200	3.33×10^{-1} to 1.67×10^{-2}	-0.96±0.02	7,7b
200-400	1.67×10^{-1} to 2.86×10^{-2}	-0.93±0.02	7,7c

4.1.3 Variation of the microcomponent concentration

It has been stated (section 2.1.2) that the concentration of the macrocomponent ion should be very much greater than the microcomponent ion concentration. This statement gives no indication of the optimum ratio of the concentrations of the two ions. Experiments were conducted, with anionic and cationic systems, to obtain, by comparison of the measured charges with the recognised values, a macrocomponent to microcomponent concentration ratio below which the above restriction breaks down.

Potassium and chloride ions were once again the ions whose charge was to be determined. The concentration of the microcomponent ion (sodium or sulphate) was varied from trace levels ($\sim 10^{-10}$) to concentrations equivalent to that of the macrocomponent ion (10^{-2} M).

The charges listed in Table 5 indicate that a macrocomponent to microcomponent concentration ratio as low as circa 10^{2}:1 can be tolerated before the restrictions of section 2.1.2 are invalidated.

It was predicted (section 2.3.1) that an increase in the microcomponent concentration which was large enough to invalidate the condition that the concentration of the macrocomponent ion must be very much greater than the concentration of the microcomponent ion would lead to a curving of the double logarithm plot of distribution coefficient versus macro-ion concentration. This effect was observed (figures 8b, c and 9b, c) in determinations where a ratio

of less than 10^2:1 was used. Charges calculated from these experiments were higher than the recognised values for the potassium and chloride ions.

TABLE 5

Variation of the apparent charge with microcomponent concentration

Anion-exchange resin:- Dowex 1X8, 50-100 mesh

Cation-exchange resin:- Dowex 50WX8, 50-100 mesh

Macrocomponent concentration range (moles/litre)	Microcomponent concentration (moles/litre)	Apparent charge	Appendix and figure
Chloride ion (as NaCl)	Sulphate ion (as $Na_2{}^{35}SO_4$)		
7.14×10^{-1}	$\sim 10^{-10}$	-0.96 ± 0.03	8, 8a
	3.0×10^{-2}	-2.1 ± 0.2	8, 8b
to	3.0×10^{-3}	-1.3 ± 0.1	8, 8c
	3.0×10^{-4}	-0.96 ± 0.04	8, 8d
1.67×10^{-2}	3.0×10^{-5}	-0.96 ± 0.02	8, 8e
Potassium ion (as KCl)	Sodium ion (as $^{22}NaCl$)		
1.00×10^{-1}	$\sim 10^{-10}$	$+1.03 \pm 0.02$	9, 9a
	1.0×10^{-2}	$+1.49 \pm 0.02$	9, 9b
to	5.0×10^{-3}	$+1.3 \pm 0.1$	9, 9c
	1.0×10^{-3}	$+1.06 \pm 0.03$	9,9d
4.00×10^{-3}	1.0×10^{-4}	$+1.02 \pm 0.04$	9, 9e

4.1.4 Variation of the apparent charge with solution concentration and resin crosslinkage

Measurement of the equivalent volumes (Appendix 4) of a number of ion-exchange resins over a wide range of electrolyte concentrations (10^{-2} to 1.0 M) showed that changes in the equivalent volume were dependent on the divinylbenzene content (degree of crosslinkage) of the resin and the concentration of the external solution. The equivalent volumes of resins with a moderately high divinylbenzene content remained essentially constant over the electrolyte concentration ranges investigated. With resins of low divinylbenzene content significant variations in equivalent volume were observed.

To examine the effect of changes in equivalent volume with resins of differing swelling ability and with alterations of the concentration of the external solution, experiments were set up to measure the charges of the two simple ions, chloride and potassium. Ion-exchange resins with 1% and 2-3% divinylbenzene were used and the results obtained were compared with those from the model systems where the resins had a divinylbenzene content of 8%. The concentration ranges of the external solutions were similar to those used for the model systems. Charges measured under the above conditions, together with charges obtained from the model systems, are recorded in Table 6.

TABLE 6

Variation of the apparent charge with changes in resin swelling

Resin	Macrocomponent concentration range (moles/litre)	Microcomponent concentration (moles/litre)	Apparent charge	Appendix and figure
	Chloride ion (as NaCl)	Sulphate ion (as $Na_2{}^{35}SO_4$)		
Dowex 1X8	7.14×10^{-1} to 1.67×10^{-2}	$\sim 10^{-10}$	-0.96 ± 0.02	10, 10a
Dowex 1X1	1.67×10^{-1} to 1.67×10^{-2}	$\sim 10^{-10}$	-1.02 ± 0.01	10, 10b
Dowex 1X1	6.92×10^{-1} to 1.67×10^{-2}	$\sim 10^{-10}$	-1.25 ± 0.08	10, 10b
De-Acidite FF (SRA 63) 2-3% DVB	6.67×10^{-1} to 1.67×10^{-2}	$\sim 10^{-10}$	-1.02 ± 0.02	10, 10c
	Potassium ion (as KCl)	Sodium ion (as $^{22}NaCl$)		
Dowex 50WX8	4.00×10^{-1} to 4.00×10^{-3}	$\sim 10^{-10}$	$+1.03 \pm 0.02$	11, 11a
Dowex 50WX1	1.00×10^{-1} to 4.00×10^{-3}	$\sim 10^{-10}$	$+1.00 \pm 0.02$	11, 11b
Dowex 50WX1	6.00×10^{-1} to 4.00×10^{-3}	$\sim 10^{-10}$	$+1.09 \pm 0.07$	11, 11b

The resins with 8% divinylbenzene showed no variation in specific volume (Appendix 4) with changes in the external solution concentration between 1.0×10^{-2} and 1.0 M. As a result changes in concentration over this range had no effect on the measured charges.

Experiments conducted with resins of very low (1%) divinylbenzene content gave double logarithm plots of distribution coefficient versus concentration which were curved when the macrocomponent concentration was greater than 1.0×10^{-1} M with the result that the calculated charge was larger than expected. Concentrations less than 1.0×10^{-1} M did not effect the slope of the double logarithm plot and the charges obtained for the chloride and potassium ions were as accurate as those obtained from the model systems.

For ion-exchange resins with a divinylbenzene content intermediate between 1% and 8% (that is 2-3%) the measured charges were the same, within the experimental error, as those calculated with the model systems. High concentrations ($> 1.0 \times 10^{-1}$ M) of macrocomponent ion did not alter the slope of the calculated line (figure 10c) or the charge obtained from this slope.

The apparent charge on an ion, as measured by the inverse batch equilibrium method, can therefore be affected by the divinylbenzene content of the resin used. If the degree of crosslinking is low the specific volume of the resin varies at high solution concentrations of the macrocomponent ion and the conditions governing the setting

up of equation (1) are violated. This, in turn, leads to a non-linearity of the double logarithm plot of distribution coefficient versus concentration and a subsequent increase in the apparent charge.

4.1.5 Further experiments with simple ions

Values obtained for the potassium and chloride ions (Table 3) indicate that the inverse batch equilibrium method of charge determination can be applied to the measurement of the charges of these simple ions. The method has also been applied to two other simple ions, the iodide ion and the magnesium ion.

The equilibrium system set up to measure the charge of the iodide ion consisted of Dowex 1X8 resin, pre-equilibrated with iodide solution, in contact with solutions of sodium iodide containing trace amounts of sulphate ion, labelled with sulphur-35. Table 7 includes the experimental conditions for this determination together with the charge calculated for the iodide ion in aqueous solution.

TABLE 7

Measurement of the charge of the iodide ion

Anion-exchange resin:- Dowex 1X8, 50-100 mesh.

Macrocomponent (iodide ion) concentration range (moles/litre)	Microcomponent (sulphate ion) concentration (moles/litre)	Apparent charge	Appendix and figure
5.81×10^{-1} to 1.95×10^{-2}	$\sim 10^{-10}$	-0.99 ± 0.02	12, 12

The charge of minus one obtained from this experiment agrees with the accepted value for the iodide ion. This, together with the value of minus one already found for the charge on the chloride ion, indicates that the inverse batch method is suitable for application to simple, negatively charged ions in solution.

Investigations of the charge of the magnesium ion in solution were carried out under similar conditions to the experiments conducted for the model systems of cations. A major difference was the choice of microcomponent ion; sodium-22 in the model systems, caesium-137 and cerium-144 in this case.

The suitability of the microcomponent cations was checked by measuring the charge of the potassium ion with solutions containing trace concentrations of caesium-137 and cerium-144. The values obtained with these ions were compared with that found from the model system where sodium-22 was used as the microcomponent. Table 8 lists the charge of the potassium ion as calculated from the above experiments.

From the Table (p.36) it can be seen that caesium is a suitable ion to use as the competing microcomponent ion while cerium(III) is not. Cerium-144 was provided as cerium(III) chloride in hydrochloric acid (1 M) and as the potassium ion was present in potassium chloride solutions it seems that chloro complexes of cerium have been formed. Complexes of this type have been reported [43] in the literature.

The presence of chloro complexes of cerium violates

one of the basic requirements for the successful application of equation (13). Infringement of the condition that the charges of the competing ions must remain constant throughout the experiment leads to errors in the solution of equation (14) because the charge of the microcomponent ion is not known.

TABLE 8

Comparison of the charges obtained for the potassium ion with various microcomponent cations

Cation-exchange resin:- Dowex 50WX8, 50-100 mesh.

Potassium ion concentration range (moles/litre)	Microcomponent ion concentration (moles/litre)	Apparent charge	Appendix and figure
4.00×10^{-1} to 4.00×10^{-3}	$^{22}Na^{+}$; $\sim 10^{-10}$	$+1.04 \pm 0.02$	6, 6a
4.00×10^{-1} to 4.00×10^{-3}	$^{137}Cs^{+}$; $\sim 10^{-10}$	$+1.01 \pm 0.06$	13, 13a
3.60×10^{-1} to 2.40×10^{-3}	$^{144}Ce(III)$; $\sim 10^{-10}$	$+5.8 \pm 0.8$	13, 13c

In spite of the results of these experiments it was decided to measure the charge of the magnesium ion with caesium-137 and with cerium-144 as the microcomponent ions. Since the magnesium was present in magnesium perchlorate solutions it was thought that chloro complexes of cerium would not form.

The results of these experiments are given in Table 9.

TABLE 9

Measurement of the charge of the magnesium ion

Cation-exchange resin:- Dowex 50WX8, 50-100 mesh.

Magnesium ion concentration range (moles/litre)	Microcomponent ion concentration (moles/litre)	Apparent charge	Appendix and figure
3.49×10^{-1} to 3.49×10^{-3}	$^{137}Cs^{+}$; $\sim 10^{-10}$	$+1.80 \pm 0.07$	13, 13b
4.19×10^{-1} to 2.53×10^{-3}	$^{144}Ce(III)$; $\sim 10^{-10}$	$+3.8 \pm 0.8$	13, 13d
4.19×10^{-1} to 3.49×10^{-2}	$^{144}Ce(III)$; $\sim 10^{-10}$	$+2.37 \pm 0.09$	13, 13d

With caesium-137 as the microcomponent ion the apparent charge of the magnesium ion was close to the expected value of plus two while the charge measured with cerium-144 as the microcomponent was much greater than this value.

Two straight lines were drawn to fit the experimentally determined points in the graph (figure 13d) of the logarithm of the distribution coefficient of cerium(III) against the logarithm of the magnesium ion concentration. The line drawn through all the points on the graph had a small slope and the apparent charge of the magnesium ion, as calculated from the slope of this line, was much greater than expected. Another line, drawn to include only the points which corresponded to magnesium ion concentrations of greater than 3.49×10^{-2} M, resulted in a charge which was much

closer to the known value of plus two.

A possible explanation is that chloro complexes have been formed by the radioactive cerium(III) which was supplied as a solution in hydrochloric acid (1 M). At higher concentrations of magnesium perchlorate the cerium and chloride ions are not able to form complexes as readily because of the large number of non-complexing ions in solution. The slope of the double logarithm plot of the cerium distribution coefficient versus the magnesium ion concentration is increased and the calculated charge of the magnesium ion approaches the recognised value of plus two.

4.1.6 The effect of resin capacity

The exchange capacity (dry) of all ion-exchange resins was measured (Appendix 3) in an attempt to assess the effect of different capacities on the apparent charge of the macrocomponent ion. It was found that the capacity varied with the resin and that it was closely connected to the divinylbenzene content of the resin. The resins which were used for the model systems contained 8% divinylbenzene and had the lowest capacity for exchange while those resins with 1% divinylbenzene had much higher capacities.

As a very low resin capacity (section 2.3.4) is necessary to invalidate the restrictions imposed (section 2.1.2) by the theory of this method the resins which should have been most affected were those which were used in the model systems. The charges calculated with these resins (section 4.1.1) agreed with the known values of the

macrocomponent ions and it must be assumed that their capacities were not low enough to alter the measured charges. Resins with lower divinylbenzene content, and correspondingly higher capacities, should not have caused any variations in the measured charges. The changes that did occur (section 4.1.4) were attributed to variations in the equivalent volumes of the resins.

4.1.7 Determination of the charge of a complex ion

The results obtained so far (Tables 3-9) indicate that this method of charge determination may be used to measure the charges of simple ions in aqueous solution . To evaluate the possible extension of the method to complex ions the charge of the tris(ethylenediamine)nickel(II) cation was measured. The charge of this ion is known to be plus two.

Each determination was carried out with a series of solutions of the tris(ethylenediamine)nickel(II) ion, $Ni(en)_3^{2+}$, containing one of the radioisotopes, sodium-22, calcium-45, or caesium-137 as cationic microcomponent in equilibrium with a cation-exchange resin which had been pre-equilibrated with the complex ion. The resins used were Dowex 50WX8, Dowex 50WX4 and Amberlite CG 120. Table 10 lists the experimental conditions and the results of these determinations.

TABLE 10

Measurement of the charge of the tris(ethylenediamine)nickel(II) ion

Resin	Nickel concentration range (moles/litre)	Microcomponent ion concentration (moles/litre)	Apparent charge	Appendix and figure
Dowex 50WX8	7.83×10^{-2} to 7.83×10^{-4}	$^{22}Na^{+}$; $\sim 10^{-10}$	$+3.3 \pm 0.9$	14, 14b
Dowex 50WX4	3.91×10^{-2} to 3.13×10^{-4}	$^{22}Na^{+}$; $\sim 10^{-10}$	$+2.08 \pm 0.08$	14, 14a
Dowex 50WX4	7.83×10^{-2} to 1.57×10^{-3}	$^{137}Cs^{+}$; $\sim 10^{-10}$	$+2.0 \pm 0.4$	14, 14c
Amberlite CG 120 8% DVB	9.54×10^{-2} to 9.54×10^{-4}	$^{22}Na^{+}$; $\sim 10^{-10}$	$+3.3 \pm 0.5$	15, 15a
Amberlite CG 120 8% DVB	7.83×10^{-2} to 7.83×10^{-4}	$^{137}Cs^{+}$; $\sim 10^{-10}$	$+3.5 \pm 0.5$	15, 15b
Amberlite CG 120 8% DVB	9.54×10^{-2} to 9.54×10^{-4}	$^{45}Ca^{2+}$; $\sim 10^{-10}$	$+2.0 \pm 0.1$	16, 16

With Dowex 50WX8 resin and sodium-22 as the microcomponent the observed charge was almost three. Similar values were recorded for Amberlite CG 120 resin with sodium-22 and caesium-137 as the trace ions. The apparent charges obtained from the experiments with Dowex 50WX4 (sodium-22 and caesium-137 as microcomponent ions) were very close to the theoretical value of plus two, as was the charge found with Amberlite CG 120 and calcium-45 as the microcomponent.

With caesium-137 the correlation coefficient for the line drawn through the experimental points was 0.91 which indicates that the points do not constitute a straight line (figure 14c). This,together with the large error in the calculated charge, showed that the value found in this experiment was not accurate.

The above results indicate that the value of the apparent charge is dependent on the resin crosslinkage and the nature of the microcomponent ion.

With the highly crosslinked resins Dowex 50WX8 and Amberlite CG 120 it is possible that the tris(ethylenediamine)-nickel(II) ion, which has a diameter of approximately 6 Angstrom units (as found by summing the ionic and covalent radii[44] of the constituent atoms), is large enough to cause partial exclusion of the sodium and caesium ions from the resin matrix. The slope of the double logarithm plot is therefore altered and the apparent charge calculated from this slope does not correspond to the expected value of plus two.

On the other hand calcium-45, with a charge of plus two and a relatively small radius[44] (0.99 Angstrom), is able to compete more strongly with the tris(ethylenediamine)nickel(II) ion, than either sodium-22 or caesium-137, for sites on the resin. As a result the charge of the complex ion calculated from the distribution measurements with the calcium ion as microcomponent and a highly crosslinked resin, Amberlite CG 120, agrees with the known value of plus two. This compares favourably with the results obtained with sodium and caesium as

the microcomponent ions which gave values of approximately three for the same complex ion measured under similar conditions (figure 14a, 15a, b).

Dowex 50WX4 is a more open resin than either Dowex 50WX8 or Amberlite CG 120 owing to its lower divinylbenzene content. With this resin both sodium-22 and caesium-137 can penetrate the resin matrix freely and yield charges for the complex ion which are close to the expected value (although that obtained with caesium-137 seems inaccurate because of the low correlation coefficient of 0.91 and large error in the charge of 2.0 $\pm$ 0.4).

Summarizing, the results of these experiments show that the method can be used to measure the charge of a mononuclear complex ion provided that the ion-exchange resin and the microcomponent ion are chosen so as to facilitate the attainment of an equilibrium between the microcomponent and the complex ions at a position that heavily favours neither ion.

4.1.8 Polymeric ions

The dichromate ion

The dichromate ion ($Cr_2O_7^{2-}$) is one of the simplest polymeric ions known. Measurement of the charge of this ion (which is known to be minus two) seemed to be a good test of the applicability of the inverse batch equilibrium method to the determination of the charges of polymeric ions in solution.

Under certain conditions polymeric chromate ions

other than dichromate can exist[45]. Owing to the presence of these ions a concentration range had to be chosen in which the dichromate ion was the only polyanion present. Martens and Carpeni[46] have determined the concentration ranges in which each of the polymeric chromate ions predominates. Their results are reproduced in Table 11.

TABLE 11

The occurrence of chromate anions in solution[46]

Chromium trioxide concentration (C) (moles/litre)	Predominant ion(s)
$10^{-2} > C$	$HCrO_4^-$
$10^{-1} > C > 10^{-2}$	$2HCrO_4^- = Cr_2O_7^{2-} + H_2O$
$1.5 > C > 10^{-1}$	$Cr_2O_7^{2-}$
$3.5 > C > 1.5$	$3Cr_2O_7^{2-} + 2H^+ = 2Cr_3O_{10}^{2-} + H_2O$
$7.5 > C > 3.5$	$Cr_3O_{10}^{2-}$
$10 > C > 7.5$	$4Cr_3O_{10}^{2-} + 2H^+ = 3Cr_4O_{13}^{2-} + H_2O$

By mixing solutions of chromium trioxide and sodium dichromate a series of solutions of chromium(VI) were prepared. To each of these solutions hexacyanocobaltate(III) ion, labelled with cobalt-60, was added as the microcomponent ion and the radioactively labelled solutions were placed in contact with Dowex 1X8 which had been pre-equilibrated with the dichromate solutions. The conditions under which the distribution measurements were carried out are given in Table 12, together with the apparent charge on the dichromate

ion.

TABLE 12

The charge of the dichromate ion

Anion-exchange resin:- Dowex 1X8, 100-200 mesh.

pH of test solutions:- 1.55.

Chromium(VI) concentration range (moles/litre)	Microcomponent concentration (moles/litre)	Apparent charge	Appendix and figure
3.81×10^{-1} to 3.40×10^{-2}	$^{60}Co(CN)_6^{3-}$; $\sim 10^{-6}$	-2.00 ± 0.07	17, 17

The apparent charge of minus two, which corresponds to the known value of the charge of this ion, indicates that the method is suitable for the measurement of the charge of a polyanion provided that the concentration range and pH are chosen so that the ion under investigation is the predominant ion in solution.

The beryllium hydrolysis polymer

As stated previously (section 1.3) the nature of the predominant ion in a slightly acidic beryllium solution has been the subject of contention for many years. The inverse batch equilibrium method of charge determination, which had proved successful in its application to a simple polymeric ion, was now used in an attempt to measure the charge of this ion and thereby seek evidence for the formula proposed by Kakihana and Sillen[7].

Beryllium perchlorate solutions were prepared with

concentrations in the range 8.02×10^{-2} to 2.24×10^{-2} M. The pH of the solutions was adjusted to 5.5 and calcium ion ($^{45}Ca^{2+}$) added as the microcomponent. Each solution was placed in contact with cation-exchange resin, pre-equilibrated with the appropriate beryllium solution, and the two phases were mixed for fourteen days. They were then separated and samples taken from the solution phase for analysis by radioactive counting. Table 13 lists the conditions under which the equilibrations were carried out together with the apparent charge of the predominant beryllium ion.

TABLE 13

The charge of the polymeric beryllium ion in slightly acidic solutions

Cation-exchange resin:- Amberlite CG 120, 8% DVB.

pH of solutions:- 5.50

Beryllium concentration range (moles/litre)	Calcium ion concentration (moles/litre)	Apparent charge	Appendix and figure
8.02×10^{-2} to 2.24×10^{-2}	$\sim 10^{-10}$	$+3.03 \pm 0.04$	18, 18

Accepting that there is only one predominant ion under the above conditions[7], the charge of this ion was found to be plus three. One of the ions $Be_3(OH)_3^{3+}$, Be_2OH^+ or $Be_6(OH)_9^{3+}$ must therefore be the major species in the beryllium solutions.

Previous work in these laboratories[6] has shown that the beryllium species on the resin has a metal to charge ratio of one and this would indicate the ion to be $Be_3(OH)_3^{3+}$. For beryllium solutions Kakihana and Sillen[7] have developed an equation whereby the concentrations of each of the species at a known total concentration of beryllium can be calculated. With this equation the ion $Be_3(OH)_3^{3+}$ was proposed as the principal ion in solutions having beryllium concentrations similar to those used in the above experiment. The ion $Be_6(OH)_9^{3+}$, mentioned by Lanza and Carpeni[21], was not present but it was suggested that the ion Be_2OH^{3+} might occur at a very low concentration.

Consideration of the previous investigations, together with the work presented herein, leads to the conclusion that the trimeric ion $Be_3(OH)_3^{3+}$ is the sole species at pH 5.5 in beryllium perchlorate solutions (8.02×10^{-2} to 2.24×10^{-2} M).

4.2 Suggestions for Future Work

Application of this method of charge determination to simple ions has shown that, provided the theoretical restrictions are imposed, the measured charge of an ion corresponds to the known value of that ion. The method has been extended to complex and polymeric ions, and with the correct choice of competing ions and resins the charges of these ions can also be determined. These investigations show that the method should be applicable to the measurement of the charge of any ion provided that it predominates in solution.

Ionic compounds to which this method could be applied include the isopoly- and heteropoly-, molybdates, germanates, vanadates and tungstates. The metal to charge ratios[47] ("R" values) of these ions have been measured, and charge determination would provide the empirical formulae of these ions in solution.

SECTION 5

CONCLUSION

A new method for ionic charge determination has been developed and successfully tested on a number of simple, complex and polymeric ions (K^+, Mg^{2+}, Cl^-, I^-, $Ni(en)_3^{2+}$, $Cr_2O_7^{2-}$). In each case the known charge values have been reproduced with high accuracy provided that a number of important experimental conditions are observed. These are discussed below. The technique has been named the "inverse batch equilibrium method" since the equilibrations are carried out batchwise with the ion of unknown charge as the macro-concentration component and the species of known charge present as the micro-concentration competitor usually, but not necessarily, at radioactive tracer level.

The theory of the method imposes a number of restrictions on the experimental conditions of the determination and a part of this work has been to set broad limits to the various possible deviations from ideality. Several important factors emerged from this study.

The macrocomponent to microcomponent concentration ratio is critical in that it controls the concentration of the macrocomponent in the resin phase. A ratio of lower than circa 10^2:1 caused a substantial and unacceptable variation in the apparent charge of the "unknown" ion.

Resins which had a very open structure (low divinylbenzene content) were prone to swelling changes between different concentrations in the one determination and caused the apparent charge to exceed the correct value. This was a result of the change in electrolyte penetration of the resin matrix. For the

same reason, variation of the concentration of the macrocomponent in the external solution over a wide range had a marked effect on the charges measured with these resins, whereas with resins of high crosslinkage there was no noticeable change.

The effect of the mesh size on the measured charge was also investigated. It was shown that the charge of the chloride ion did not vary with resins of differing mesh size and it is assumed that, provided sufficient time is allowed for equilibration, this will not be an important factor.

The use of ions of known charge which have the potential to form complexes should also be avoided. Because of the availability of cerium(III) and its high ionic charge it was used as the microcomponent in several experiments. It seems that this choice was injudicious as the apparent charges of the potassium and magnesium ions calculated from the distribution measurements with cerium(III) were much higher than the expected values. This error was probably caused by the formation of chloro-complexes which altered the charge of the cerium(III) species and, as the theory demands that the charges of the ions must not vary throughout the experiment, the wrong values were obtained.

The method was applied finally to the major ionic species formed in beryllium perchlorate solutions. A value of plus three was calculated for the charge of this ion which, in conjunction with other evidence, confirmed the presence of the ion $Be_3(OH)_3^{3+}$ as the predominant species in these solutions.

SECTION 6

APPENDICES

Notes to the Appendices and Figures Therein

(i) All logarithms are to the base 10.

(ii) The following abbreviations have been used for the distribution coefficients of the various radioisotopes.

(a) D_S:- sulphur-35 as the sulphate ion (SO_4^{2-}).

(b) D_{Na}:- sodium-22 as the sodium ion (Na^+).

(c) D_{Cs}:- caesium-137 as the caesium ion (Cs^+).

(d) D_{Ce}:- cerium-144 as the cerium ion (Ce^{3+}).

(e) D_{Ca}:- calcium-45 as the calcium ion (Ca^{2+}).

(f) D_{Co}:- cobalt-60 as the hexacyanocobaltate(III) ion ($Co(CN)_6^{3-}$).

(iii) The concentrations of the macrocomponent ions are represented by the following symbols.

(a) C_{Cl}:- concentration of the chloride ion (Cl^-).

(b) C_K:- concentration of the potassium ion (K^+).

(c) C_I:- concentration of the iodide ion(I^-).

(d) C_{Mg}:- concentration of the magnesium ion (Mg^{2+}).

(e) C_{Ni}:- concentration of the tris(ethylenediamine)-nickel(II) ion ($Ni(en)_3^{2+}$).

(f) C_{Cr}:- concentration of chromium(VI) in solutions of sodium dichromate and chromium trioxide.

(g) C_{Be}:- concentration of beryllium in beryllium perchlorate solutions.

(iv) Each distribution coefficient quoted in the Appendices is the mean value of a number of determinations at the one macrocomponent concentration and as such the errors have been included. In most cases these errors have not been drawn on

the figures as they are small enough to be within the open circles used to represent each point.

(v) In several figures (for example 8b, 9b) straight lines have been drawn through sets of points which obviously lie on a curve (as can be seen by the correlation coefficients). This has been done in order to obtain, by least squares analysis, the slope of such a line and to show the resulting error in the calculated charge.

APPENDIX 1

Calculation of the Distribution Coefficient

The distribution coefficient which is a measure of the distribution of the microcomponent ion, B^x, between two phases has been defined as;

$$D_B = \frac{C_{\bar{B}}}{C_B} \qquad \ldots.(5)$$

For this equation to be applied to the method under consideration the concentrations $C_{\bar{B}}$ and C_B must be expressed in readily measurable experimental factors.

The distribution coefficient of any substance, P, may be written[48] as,

$$D_P = \frac{\% \text{ of P on resin}}{\% \text{ of P in solution}} \times \frac{\text{volume of solution(ml)}}{\text{mass of dry resin(g)}} \qquad \ldots.(15)$$

This may be applied to the inverse batch equilibrium system in that the distribution coefficient of the ion B^x may be written as,

$$D_B = \frac{\% \text{ of B on the resin}}{\% \text{ of B in solution}} \times \frac{\text{volume of solution(ml)}}{\text{mass of dry resin(g)}} \qquad \ldots.(16)$$

As B^x was present at very small concentrations ($\sim 10^{-10}$ M) estimation of the percentage of this ion on the resin and in solution was quite difficult. To overcome this difficulty the ion B^x was introduced into the system as a radioisotope, the activity of which was directly proportional to the mass of isotope present. Measurement of the radioactivity in solution, both before and after equilibration with the ion-exchange resin provided the mass of B^x in each phase.

The initial activity of the solution is defined as T_I

(counts per millilitre per unit time) and that of the solution after equilibration with an ion-exchange resin as T_E (counts per millilitre per unit time).

The mass of B^x on the resin is represented by,

$$(T_I - T_E) \cdot m_B \qquad \ldots.(17)$$

and the percentage of B^x on the resin becomes,

$$\frac{(T_I - T_E) \cdot m_B}{T_I} \qquad \ldots.(18)$$

The percentage of B^x in solution is,

$$\frac{T_E}{T_I} \cdot m_B \qquad \ldots.(19)$$

Where m_B is the initial mass of the ion B^x in solution.

Substituting equations (18) and (19) into equation (16) and simplifying the resulting equation gives the following expression for the distribution coefficient.

$$D_B = \frac{(T_I - T_E)}{T_E} \cdot \frac{v}{m} \quad \text{(millilitres/gramme)} \quad \ldots.(20)$$

where v is the volume of the solution in millilitres and m is the mass of dry resin in grammes.

All distribution coefficients listed in Appendices 5 to 18 were calculated with equation (20).

APPENDIX 2

Calculation of the Slope, Intercept and Correlation Coefficient by Least Squares Analysis[49]

(i) Slope

In the figures 5 to 18 the slope of each line was calculated with the following equation.

$$\text{slope} = \frac{n\,\Sigma xy - \Sigma x.\Sigma y}{n\,\Sigma(x)^2 - (\Sigma x)^2} \qquad \ldots.(21)$$

where, x represents the logarithm of the concentration of the macrocomponent ion.

y represents the logarithm of the distribution coefficient of the microcomponent ion.

n is the number of points used in the calculation.

(ii) Intercept

The intercept of the line with the y-axis was calculated with the formula,

$$\text{intercept} = \bar{y} - \text{slope} \cdot \bar{x} \qquad \ldots.(22)$$

where $\bar{x}$ and $\bar{y}$ represent the mean values of x and y.

(iii) Correlation Coefficient

The correlation coefficient, a measure of the distribution of the experimentally determined points about a straight line drawn through them, was calculated by applying the equation

$$\text{correlation coefficient} = \text{slope} \cdot \left(\frac{n\,\Sigma(x)^2 - (\Sigma x)^2}{n\,\Sigma(y)^2 - (\Sigma y)^2}\right)^{\frac{1}{2}} \ldots.(23)$$

Values of 1.00 indicate that the points do lie on the straight line drawn through them. A value of between 0.95 and 0.99 indicates that it is likely(but not certain) that

the points lie on a straight line, while a correlation coefficient below 0.95 indicates that the points are not evenly distributed around the straight line that has been drawn through them.

Calculation of Errors

The error in the slope of the line in each of the double logarithm plots, and subsequently the error in the apparent charge, was calculated with the formula[50]

$$\text{standard deviation} = \left(\frac{\Sigma(r)^2}{n-1}\right)^{\frac{1}{2}}$$

where, n is the number of points through which the line passes and, r is the difference between the experimental value of y and the calculated value obtained from the line drawn by least squares analysis of the points.

APPENDIX 3

Capacities of the Ion-Exchange Resins

Resin	Capacity (milliequivalents/gramme of dry resin)
Anion-exchange resins	
Dowex 1X8, 50-100 mesh	3.55
Dowex 1X8, 100-200 mesh	3.17
Dowex 1X8, 200-400 mesh	3.26
Dowex 1X1, 50-100 mesh	4.36
De-Acidite FF (SRA 71) 7-9% DVB, 100-200 mesh	2.97
De-Acidite FF (SRA 63) 2-3% DVB, 100-200 mesh	3.78
Amberlite IRA 400 3-5% DVB, 100-200 mesh	3.99
Cation-exchange resins	
Dowex 50WX8, 50-100 mesh	4.14
Dowex 50WX4, 50-100 mesh	4.54
Dowex 50WX1, 50-100 mesh	4.85
Amberlite CG 120 8% DVB 100-200 mesh	4.22
Zeo-Karb (SRC 15) 8% DVB, 100-200 mesh	4.12

APPENDIX 4

Changes in the Equivalent Volumes of Ion-Exchange Resins with Variations in the Concentration of the External Solution

Resin	Equivalent volume (millilitres/equivalent)			
Anion-exchange resins	Chloride ion concentration (moles/litre)			
	5.0×10^{-2}	1.0×10^{-1}	5.0×10^{-1}	1.00
Dowex 1X8, 50-100 mesh	700	700	700	700
Dowex 1X1, 50-100 mesh	2660	2360	1720	1570
De-Acidite FF (SRA 71) 7-9% DVB, 100-200 mesh	1030	1010	1000	1000
De-Acidite FF (SRA 63) 2-3% DVB, 100-200 mesh	1080	1060	1030	1000
Amberlite IRA 400 3-5% DVB, 100-200 mesh	660	660	660	640
Cation-exchange resins	Potassium ion concentration (moles/litre)			
	3.0×10^{-2}	9.0×10^{-2}	5.0×10^{-1}	9.0×10^{-1}
Dowex 50WX8, 50-100 mesh	470	470	470	470
Dowex 50WX4, 50-100 mesh	670	620	600	570
Dowex 50WX1, 50-100 mesh	1210	1140	940	800
Amberlite CG 120 8% DVB, 100-200 mesh	520	520	500	500
Zeo-Karb (SRC 15) 8% DVB, 100-200 mesh	520	520	520	520

APPENDIX 5

Model systems for the determination of the charge of an anion (Cl^-)

Chloride ion concentration range:- 7.14×10^{-1} to 1.67×10^{-2} M.

Sulphate ion concentration:- $\sim 10^{-10}$ M.

pH of test solutions:- neutral.

Anion-exchange resins:-

(a) Dowex 1X8, 50-100 mesh.

(b) De-Acidite FF (IP), 7-9% DVB, 100-200 mesh.

(c) Amberlite IRA 400, 3-5% DVB, 100-200 mesh.

$-\log C_{Cl}$	$\log D_S$		
	(a)	(b)	(c)
1.778	3.32 ± 0.07	3.24 ± 0.02	3.15 ± 0.06
1.484		2.72 ± 0.03	
1.477	2.75 ± 0.08		2.70 ± 0.09
1.301	2.38 ± 0.06	2.28 ± 0.02	2.40 ± 0.01
1.176	2.12 ± 0.05	1.95 ± 0.01	2.15 ± 0.02
1.097	1.96 ± 0.05	1.865 ± 0.002	1.99 ± 0.01
1.079	1.94 ± 0.03		
1.000	1.78 ± 0.05	1.617 ± 0.008	1.83 ± 0.05
0.778	1.31 ± 0.07	1.22 ± 0.02	1.33 ± 0.07
0.477	0.74 ± 0.06	0.57 ± 0.02	0.60 ± 0.05
0.301	0.26 ± 0.02	0.36 ± 0.03	0.21 ± 0.01
0.176	0.005 ± 0.001		0.05 ± 0.01
0.146	-0.057 ± 0.002	0.12 ± 0.01	0.042 ± 0.007

FIGURE 5

(compiled from Appendix 5)

Model systems for measuring the charge of an anion (Cl^-)

	slope of line (least squares fit)	apparent charge	correlation coefficient
(a)	2.08 ± 0.03	-0.96 ± 0.02	1.00
(b)	1.95 ± 0.06	-1.03 ± 0.03	1.00
(c)	2.03 ± 0.07	-0.99 ± 0.04	1.00

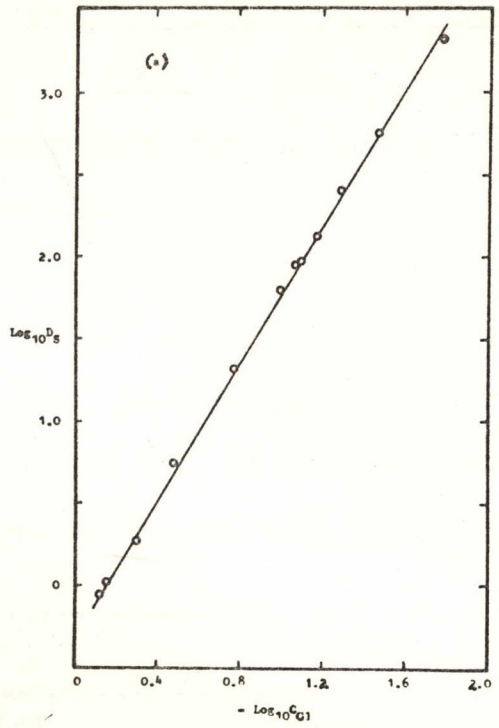
(a)
3.0
2.0
1.0
0
$Log_{10}D_S$
0
0.4
0.8
1.2
1.6
2.0
$- Log_{10}C_{Cl}$

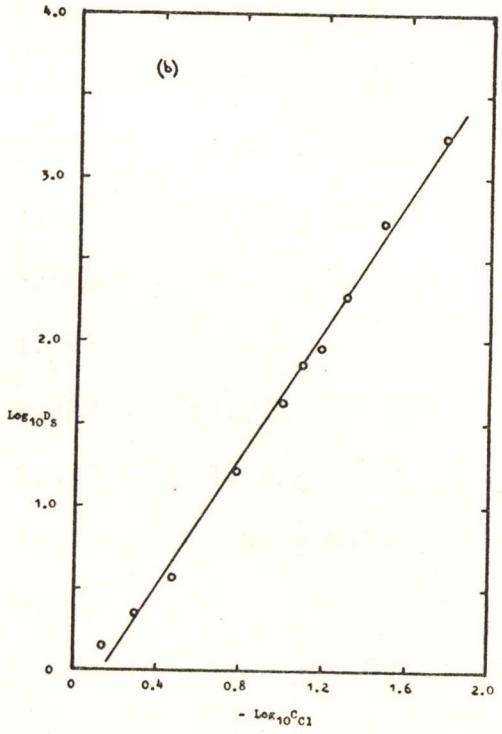
(b)
4.0
3.0
2.0
1.0
0
$Log_{10}D_S$
0
0.4
0.8
1.2
1.6
2.0
$- Log_{10}C_{Cl}$

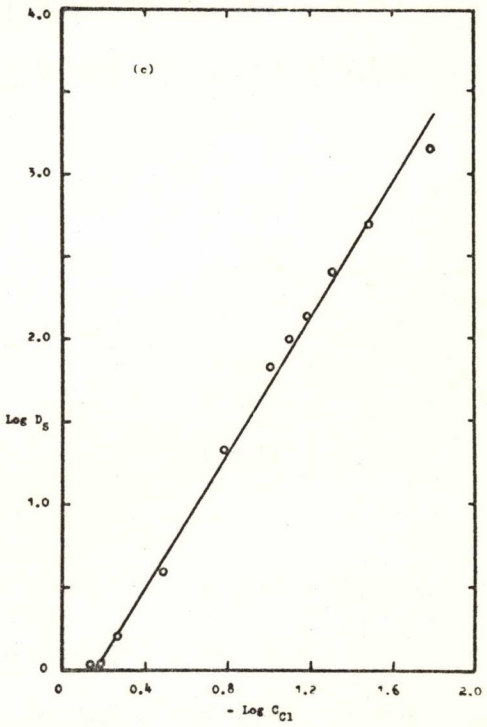
(c)
4.0
3.0
2.0
1.0
0
Log D_S
0
0.4
0.8
1.2
1.6
2.0
- Log C_{Cl}

APPENDIX 6

Model systems for the determination of the charge of a cation (K^+)

Potassium ion concentration range:- 4.00×10^{-1} to 4.00×10^{-3} M.

Sodium ion concentration:- $\sim 10^{-10}$ M.

pH of test solutions:- neutral.

Cation-exchange resins:-

(a) Dowex 50WX8, 50-100 mesh.

(b) Zeo-Karb (SRC 15), 8% DVB, 100-200 mesh.

(c) Amberlite CG 120, 8% DVB, 100-200 mesh.

$-\log C_K$	$\log D_{Na}$		
	(a)	(b)	(c)
2.398	2.839 ± 0.002	2.86 ± 0.04	2.90 ± 0.02
2.222	2.73 ± 0.04	2.68 ± 0.03	2.62 ± 0.01
2.097	2.59 ± 0.02	2.558 ± 0.006	2.60 ± 0.03
2.000	2.48 ± 0.03		
1.699	2.17 ± 0.02	2.138 ± 0.006	2.16 ± 0.02
1.398	1.89 ± 0.03	1.88 ± 0.02	1.86 ± 0.03
1.242		1.73 ± 0.02	
1.222	1.712 ± 0.007		
1.097	1.60 ± 0.02		1.572 ± 0.003
1.000	1.48 ± 0.02		
0.824			1.306 ± 0.004
0.699	1.20 ± 0.03	1.195 ± 0.007	
0.398	0.978 ± 0.008	0.864 ± 0.004	0.903 ± 0.006

FIGURE 6

(compiled from Appendix 6)

Model systems for measuring the charge of a cation (K^+)

	slope of line (least squares fit)	apparent charge	correlation coefficient
(a)	0.97 ± 0.02	+ 1.03 ± 0.02	1.00
(b)	0.99 ± 0.03	+ 1.01 ± 0.03	1.00
(c)	0.99 ± 0.04	+ 1.01 ± 0.04	1.00

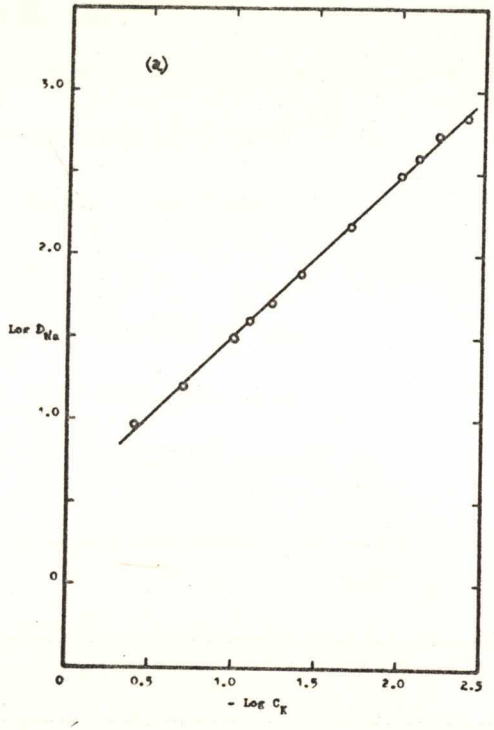
(a)
3.0
2.0
1.0
0
Log D_{Na}
0
0.5
1.0
1.5
2.0
2.5
- Log C_K

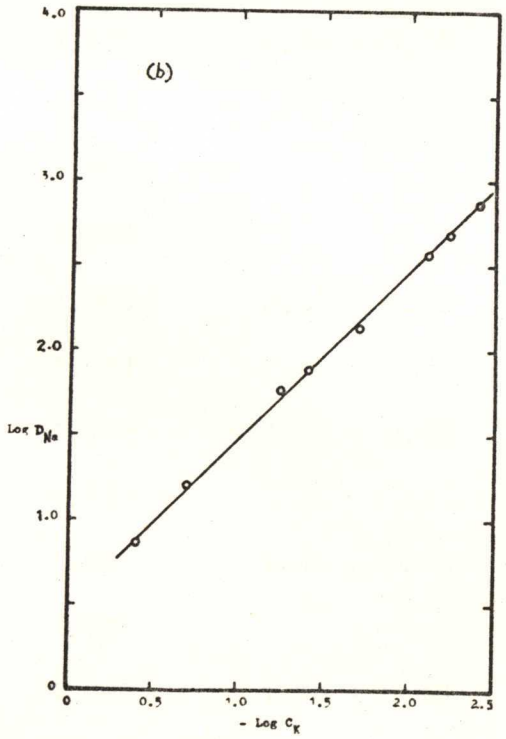
(b)
4.0
3.0
2.0
1.0
0
Log D_{Na}
0
0.5
1.0
1.5
2.0
2.5
- Log C_K

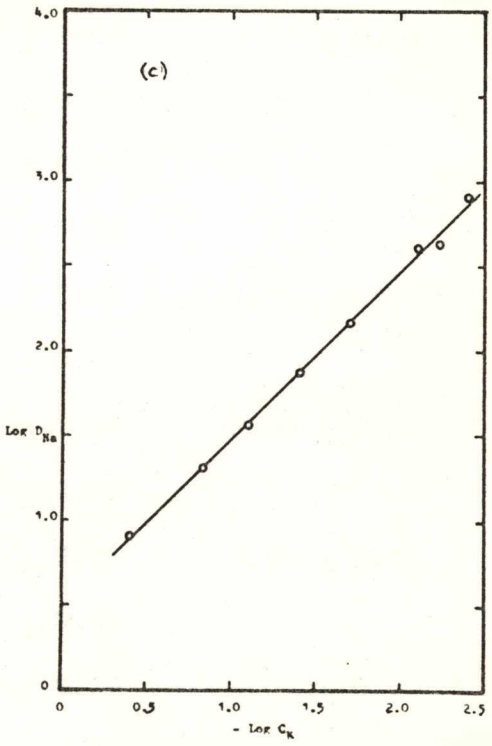
(c)
4.0
3.0
2.0
1.0
0
Log D_{Na}
0
0.5
1.0
1.5
2.0
2.5
- Log C_K

APPENDIX 7

Variation of mesh size

Chloride ion concentration range:- 7.14×10^{-1} M to 1.667×10^{-2} M.

Sulphate ion concentration:-$\sim 10^{-10}$ M.

pH of test solutions:- neutral.

Anion-exchange resins:-

(a) Dowex 1X8 50-100 mesh.

(b) Dowex 1X8 100-200 mesh.

(c) Dowex 1X8 200-400 mesh.

$-\log C_{Cl}$	$\log D_S$		
	(a)	(b)	(c)
1.778	3.32 ± 0.07	3.24 ± 0.05	3.36 ± 0.02
1.512		2.70 ± 0.05	
1.477	2.75 ± 0.08	2.66 ± 0.08	2.73 ± 0.04
1.433		2.53 ± 0.02	
1.398		2.49 ± 0.08	
1.336		2.35 ± 0.02	
1.301	2.38 ± 0.06	2.30 ± 0.04	2.374 ± 0.009
1.211		2.06 ± 0.02	
1.176	2.12 ± 0.05	2.05 ± 0.03	2.10 ± 0.01
1.132		1.86 ± 0.02	
1.097	1.96 ± 0.05	1.89 ± 0.03	1.90 ± 0.02
1.035		1.73 ± 0.03	
1.000	1.78 ± 0.05	1.67 ± 0.03	1.64 ± 0.04
0.778	1.31 ± 0.07	1.25 ± 0.007	1.23 ± 0.03
0.477	0.74 ± 0.06	0.492 ± 0.007	

	(a)
0.301	0.26 ± 0.02
0.176	0.005 ± 0.001
0.146	-0.057 ± 0.002

FIGURE 7

(compiled from Appendix 7)

The effect of mesh size on the apparent charge

	slope of line (least squares fit)	apparent charge	correlation coefficient
(a)	2.08 ± 0.03	-0.96 ± 0.02	1.00
(b)	2.09 ± 0.03	-0.96 ± 0.02	0.99
(c)	2.16 ± 0.03	-0.93 ± 0.02	1.00

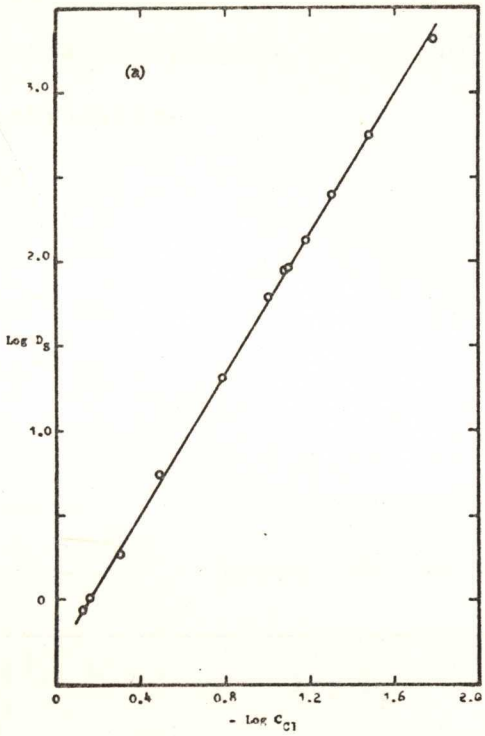
(a)
3.0
2.0
Log D_g
1.0
0
0
0.4
0.8
1.2
1.6
2.0
- Log C_{Cl}

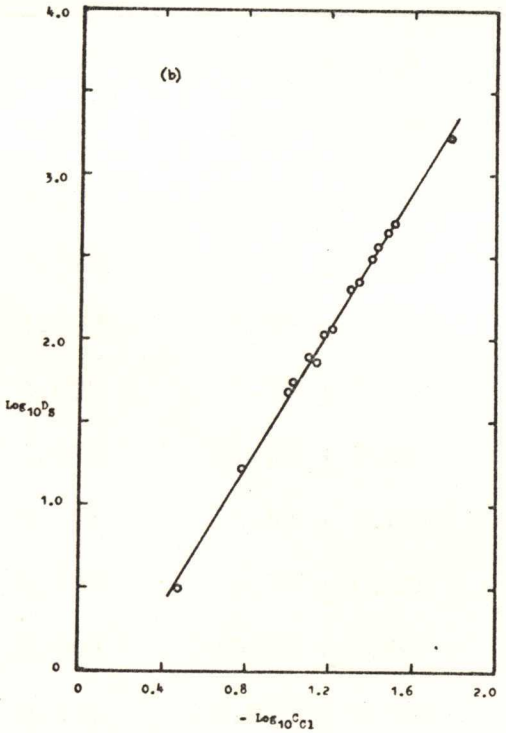
(b)
4.0
3.0
2.0
$Log_{10} D_g$
1.0
0
0
0.4
0.8
1.2
1.6
2.0
- $Log_{10} C_{Cl}$

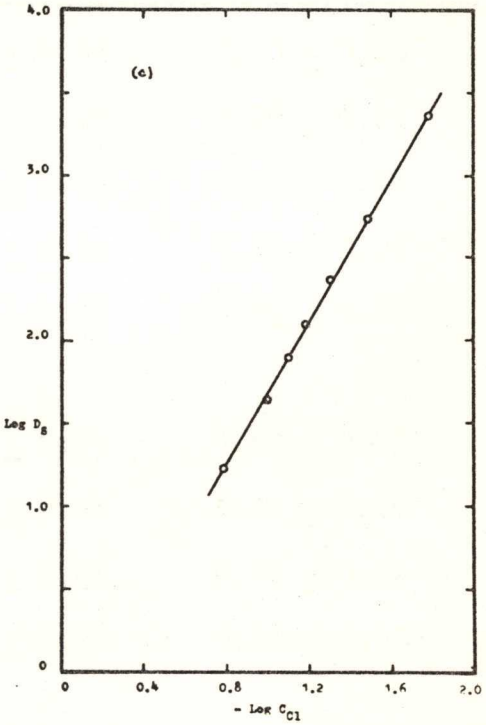
(c)
4.0
3.0
2.0
Log D_g
1.0
0
0
0.4
0.8
1.2
1.6
2.0
- Log C_{Cl}

APPENDIX 8

Variation of the microcomponent concentration (anions)

Chloride ion concentration range:- 7.14×10^{-1} to 1.67×10^{-2} M.

Sulphate ion concentration:-

(a) $\sim 10^{-10}$ M.

(b) 3.0×10^{-2} M.

(c) 3.0×10^{-3} M.

(d) 3.0×10^{-4} M.

(e) 3.0×10^{-5} M.

pH of test solutions:- neutral.

Anion-exchange resin:- Dowex 1X8, 50-100 mesh.

$-\log C_{Cl}$	$\log D_S$		
	(a)	(b)	(c)
1.778	3.32 ± 0.08	1.65 ± 0.01	2.30 ± 0.06
1.477	2.75 ± 0.09	1.43 ± 0.03	2.20 ± 0.05
1.301	2.38 ± 0.06	1.39 ± 0.03	1.99 ± 0.04
1.176	2.12 ± 0.05	1.32 ± 0.02	1.85 ± 0.03
1.097	1.96 ± 0.05	1.26 ± 0.08	1.76 ± 0.04
1.079	1.94 ± 0.03		
1.000	1.78 ± 0.05	1.11 ± 0.04	1.55 ± 0.08
0.778	1.31 ± 0.07	0.86 ± 0.03	1.20 ± 0.06
0.477	0.74 ± 0.09	0.44 ± 0.03	0.59 ± 0.04
0.301	0.26 ± 0.02	0.31 ± 0.08	0.23 ± 0.03
0.176	0.005 ± 0.001		
0.146	-0.057 ± 0.002	0.24 ± 0.04	

$\log C_{Cl}$	(d)	(e)
1.778	3.21 ± 0.03	3.25 ± 0.09
1.477	2.75 ± 0.03	2.77 ± 0.03
1.301	2.40 ± 0.01	2.39 ± 0.04
1.176	2.17 ± 0.01	2.13 ± 0.03
1.097	2.03 ± 0.01	1.97 ± 0.02
1.079		
1.000	1.823 ± 0.006	1.76 ± 0.02
0.778	1.283 ± 0.004	1.26 ± 0.04
0.477	0.618 ± 0.009	0.64 ± 0.04
0.301	0.160 ± 0.03	0.21 ± 0.07
0.176		
0.146		

FIGURE 8

(compiled from Appendix 8)

The effect of microcomponent ion concentration on the apparent charge (anions)

	slope of line (least squares fit)	apparent charge	correlation coefficient
(a)	2.08 ± 0.03	-0.96 ± 0.02	1.00
(b)	0.95 ± 0.09	-2.1 ± 0.2	0.98
(c)	1.5 ± 0.2	-1.3 ± 0.1	0.97
(d)	2.09 ± 0.08	-0.96 ± 0.04	1.00
(e)	2.09 ± 0.05	-0.96 ± 0.02	1.00

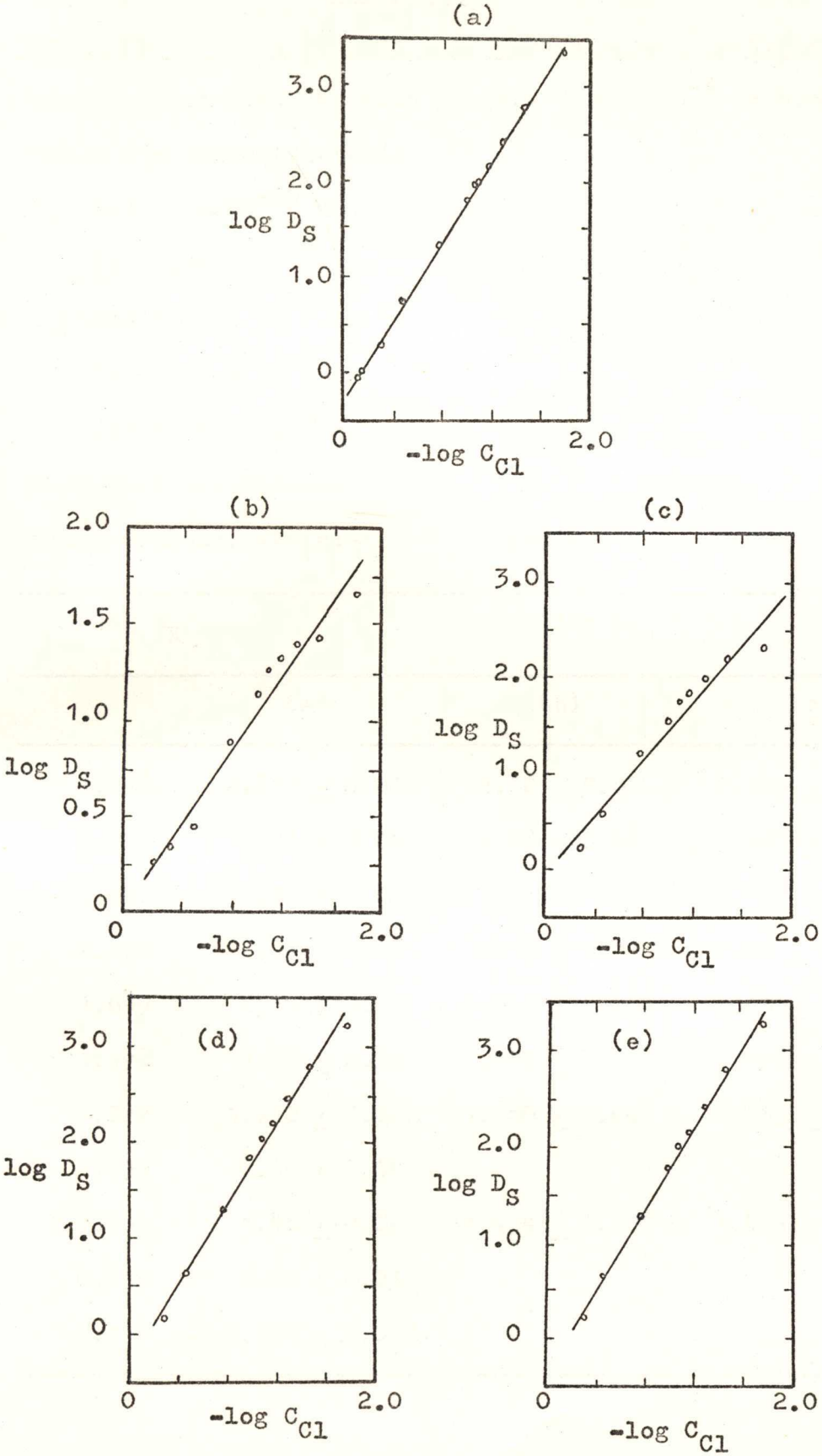
(a)
3.0
2.0
log D_S
1.0
0
0
-log C_{Cl}
2.0
(b)
2.0
1.5
1.0
log D_S
0.5
0
0
-log C_{Cl}
2.0
(c)
3.0
2.0
log D_S
1.0
0
0
-log C_{Cl}
2.0
3.0
(d)
2.0
log D_S
1.0
0
0
-log C_{Cl}
2.0
3.0
(e)
2.0
log D_S
1.0
0
0
-log C_{Cl}
2.0

APPENDIX 9

Variation of the microcomponent concentration (cations)

Potassium ion concentration range:- 4.00×10^{-3} to 4.00×10^{-1} M.

Sodium ion concentration:-

(a) $\sim 10^{-10}$ M.

(b) 1.00×10^{-2} M.

(c) 5.00×10^{-3} M.

(d) 1.00×10^{-3} M.

(e) 1.00×10^{-4} M.

pH of test solutions:- neutral.

Cation-exchange resin:- Dowex 50WX8, 50-100 mesh.

$-\log C_K$	$\log D_{Na}$		
	(a)	(b)	(c)
2.398	2.839 ± 0.002	2.32 ± 0.02	2.499 ± 0.006
2.222	2.73 ± 0.05	2.28 ± 0.01	2.401 ± 0.005
2.097	2.59 ± 0.02		
2.000	2.48 ± 0.03	2.13 ± 0.03	2.26 ± 0.02
1.699	2.17 ± 0.02	1.946 ± 0.004	2.05 ± 0.01
1.398	1.89 ± 0.03	1.742 ± 0.002	1.798 ± 0.006
1.222	1.712 ± 0.007	1.589 ± 0.007	1.639 ± 0.004
1.097	1.60 ± 0.02		
1.000	1.48 ± 0.02	1.404 ± 0.009	1.415 ± 0.009
0.699	1.20 ± 0.03		
0.398	0.978 ± 0.008		

$\log C_K$	(d)	(e)
2.398	2.76 ± 0.02	1.829 ± 0.004
2.222	2.618 ± 0.008	1.70 ± 0.01
2.097		
2.000	2.420 ± 0.003	2.45 ± 0.04
1.699	2.14 ± 0.02	2.19 ± 0.03
1.398	1.85 ± 0.02	1.891 ± 0.004
1.222	1.672 ± 0.004	1.699 ± 0.003
1.097		
1.000	1.433 ± 0.006	1.46 ± 0.03
0.699		
0.398		

FIGURE 9

(compiled from Appendix 9)

The effect of microcomponent ion concentration on the apparent charge (cations)

	slope of line (least squares fit)	apparent charge	correlation coefficient
(a)	0.97 ± 0.02	+ 1.03 ± 0.02	1.00
(b)	0.67 ± 0.04	+ 1.49 ± 0.09	0.99
(c)	0.77 ± 0.04	+ 1.30 ± 0.07	1.00
(d)	0.95 ± 0.02	+ 1.06 ± 0.03	1.00
(e)	0.98 ± 0.03	+ 1.02 ± 0.04	1.00

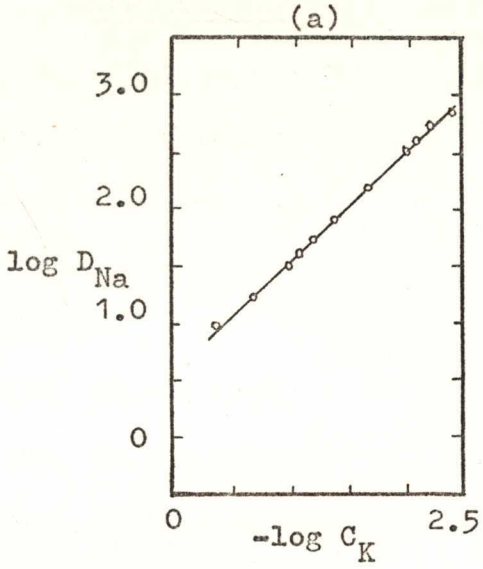
(a)
3.0
2.0
log D_{Na}
1.0
0
0
-log C_K
2.5

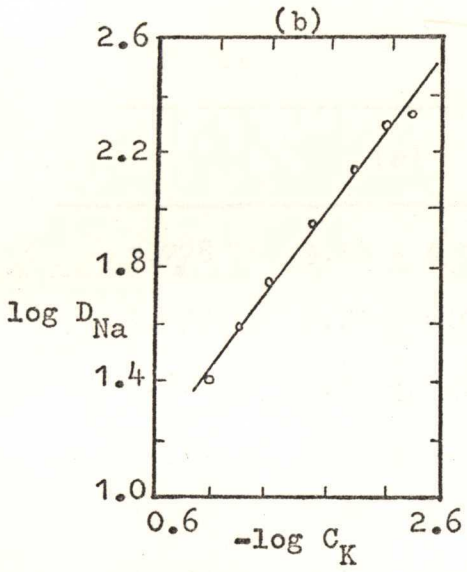
(b)
2.6
2.2
1.8
log D_{Na}
1.4
1.0
0.6
-log C_K
2.6

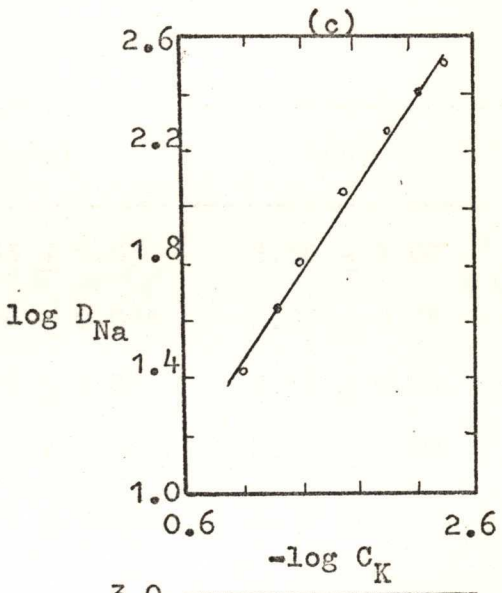
(c)
2.6
2.2
1.8
log D_{Na}
1.4
1.0
0.6
-log C_K
2.6

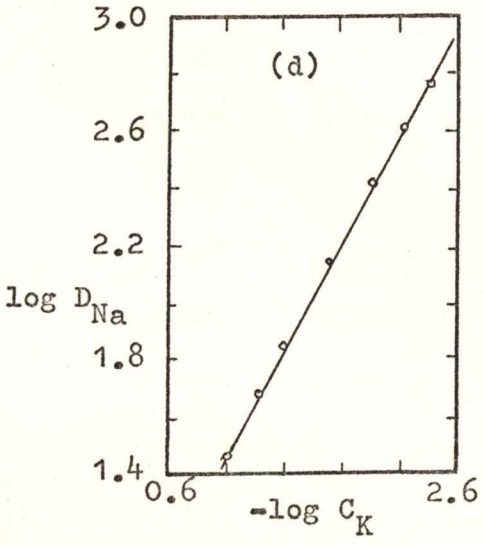
3.0
(d)
2.6
2.2
log D_{Na}
1.8
1.4
0.6
-log C_K
2.6

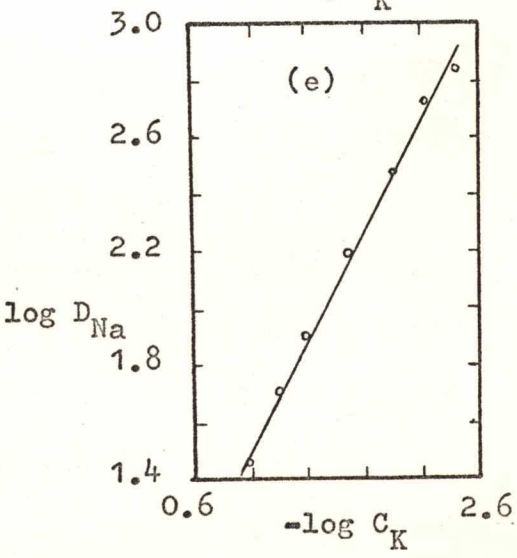
3.0
(e)
2.6
2.2
log D_{Na}
1.8
1.4
0.6
-log C_K
2.6

APPENDIX 10

The effect of resin volume on the charge (anions)

Chloride ion concentration range:- 7.14×10^{-1} to 1.67×10^{-2} M.

Sulphate ion concentration:- $\sim 10^{-10}$ M.

pH of test solutions:- neutral.

Anion-exchange resins:-

(a) Dowex 1X8, 50-100 mesh.

(b) Dowex 1X1, 50-100 mesh.

(c) De-Acidite FF (SRA 63), 2-3% DVB, 100-200 mesh.

$-\log C_{Cl}$	$\log D_S$		
	(a)	(b)	(c)
1.778	3.32 ± 0.07	3.53 ± 0.03	3.50 ± 0.07
1.477	2.75 ± 0.08	2.928 ± 0.005	2.91 ± 0.04
1.301	2.38 ± 0.06	2.57 ± 0.08	2.54 ± 0.04
1.176	2.12 ± 0.05	2.31 ± 0.03	2.25 ± 0.02
1.097	1.96 ± 0.05	2.17 ± 0.02	2.14 ± 0.02
1.079	1.94 ± 0.03		
1.000	1.78 ± 0.05	2.00 ± 0.03	1.92 ± 0.03
0.778	1.31 ± 0.07	1.59 ± 0.04	1.46 ± 0.01
0.535		1.19 ± 0.03	
0.477	0.74 ± 0.06	1.19 ± 0.04	0.84 ± 0.02
0.301	0.26 ± 0.02	1.02 ± 0.03	0.58 ± 0.02
0.176	0.005 ± 0.001		0.352 ± 0.004
0.161		0.93 ± 0.02	
0.146	-0.057 ± 0.002		0.301 ± 0.008

FIGURE 10

(compiled from Appendix 10)

The effect of crosslinkage on the apparent charge (anions)

	slope of line (least squares fit)	apparent charge	correlation coefficient
(a)	2.08 ± 0.03	-0.96 ± 0.02	1.00
(b)(n=7)	1.95 ± 0.02	-1.02 ± 0.01	1.00
(n=11)	1.6 ± 0.1	-1.25 ± 0.08	0.99
(c)	1.97 ± 0.04	-1.02 ± 0.02	1.00

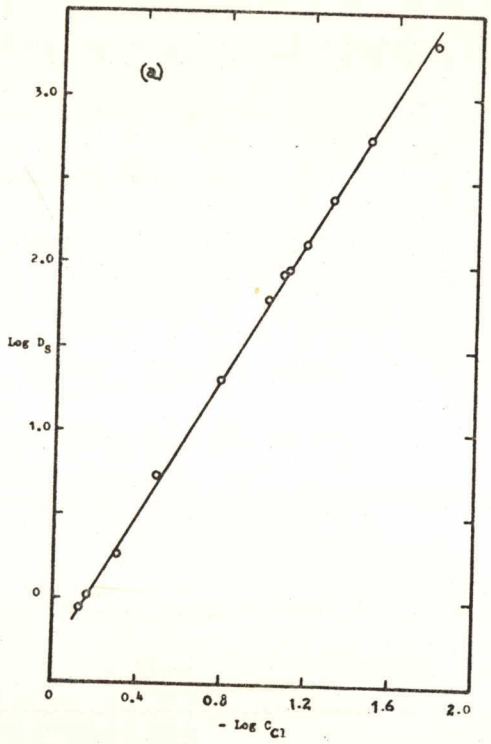
(a)
3.0
2.0
Log D_S
1.0
0
0
0.4
0.8
1.2
1.6
2.0
- Log C_{Cl}

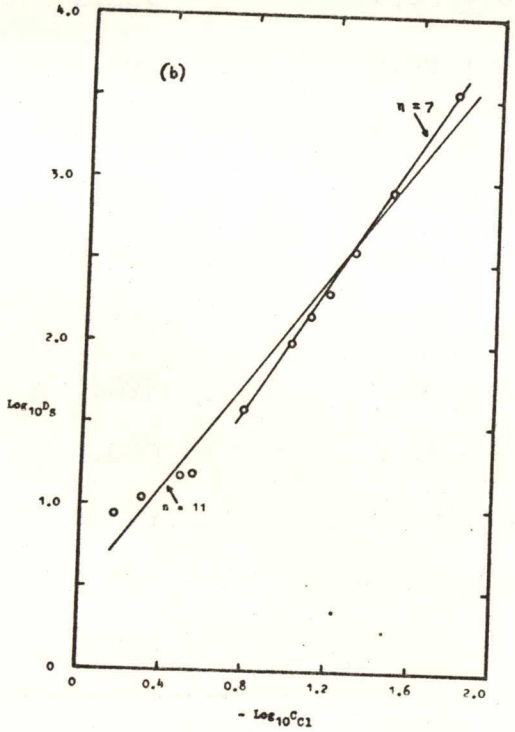
(b)
n = 7
n = 11
4.0
3.0
2.0
$Log_{10} D_S$
1.0
0
0
0.4
0.8
1.2
1.6
2.0
- $Log_{10} C_{Cl}$

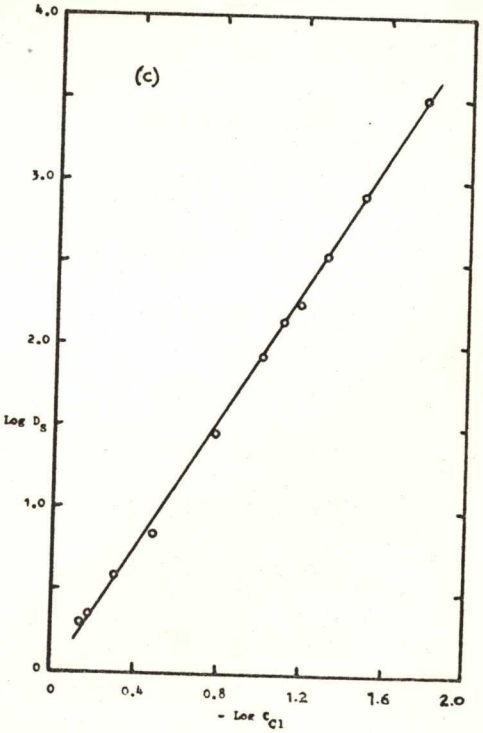
(c)
4.0
3.0
2.0
Log D_S
1.0
0
0
0.4
0.8
1.2
1.6
2.0
- Log C_{Cl}

APPENDIX 11

The effect of resin volume on the charge (cations)

Potassium ion concentration range:- 6.00×10^{-1} to 4.00×10^{-3} M.

Sodium ion concentration:- $\sim 10^{-10}$ M.

pH of test solutions:- neutral.

Cation-exchange resins:-

(a) Dowex 50WX8, 50-100 mesh.

(b) Dowex 50WX1, 50-100 mesh.

$-\log C_K$	$\log D_{Na}$	
	(a)	(b)
2.398	2.839 ± 0.002	3.10 ± 0.06
2.222	2.73 ± 0.04	2.90 ± 0.07
2.097	2.59 ± 0.02	
2.000	2.48 ± 0.03	2.65 ± 0.04
1.699	2.17 ± 0.02	2.35 ± 0.03
1.398	1.89 ± 0.03	2.07 ± 0.03
1.222	1.712 ± 0.007	1.92 ± 0.05
1.097	1.60 ± 0.02	
1.000	1.48 ± 0.02	1.67 ± 0.02
0.699	1.20 ± 0.03	1.412 ± 0.007
0.398	0.978 ± 0.008	1.270 ± 0.007
0.222		1.101 ± 0.002

FIGURE 11

(compiled from Appendix 11)

The effect of crosslinkage on the apparent charge (cations)

	slope of line (least squares fit)	apparent charge	correlation coefficient
(a)	0.97 ± 0.02	+ 1.03 ± 0.02	1.00
(b)(n=7)	0.92 ± 0.06	+ 1.09 ± 0.07	1.00
(n=10)	1.00 ± 0.02	+ 1.00 ± 0.02	1.00

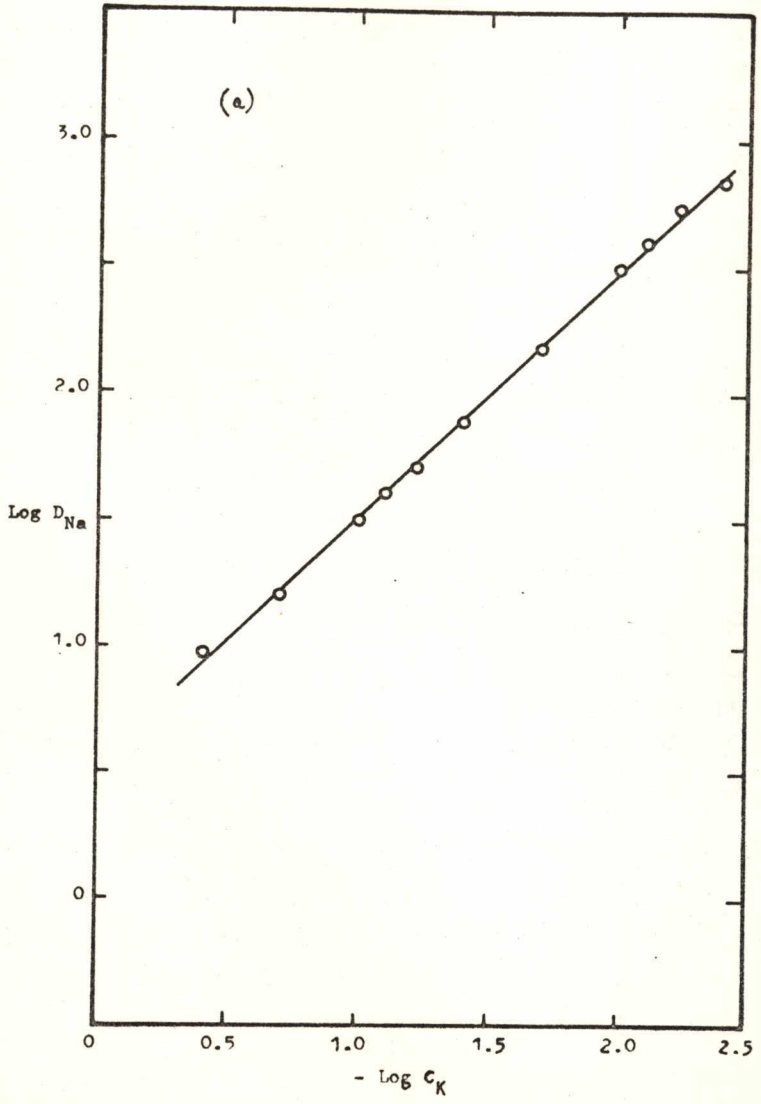
(a)
3.0
2.0
1.0
0
Log D_{Na}
0
0.5
1.0
1.5
2.0
2.5
- Log C_K

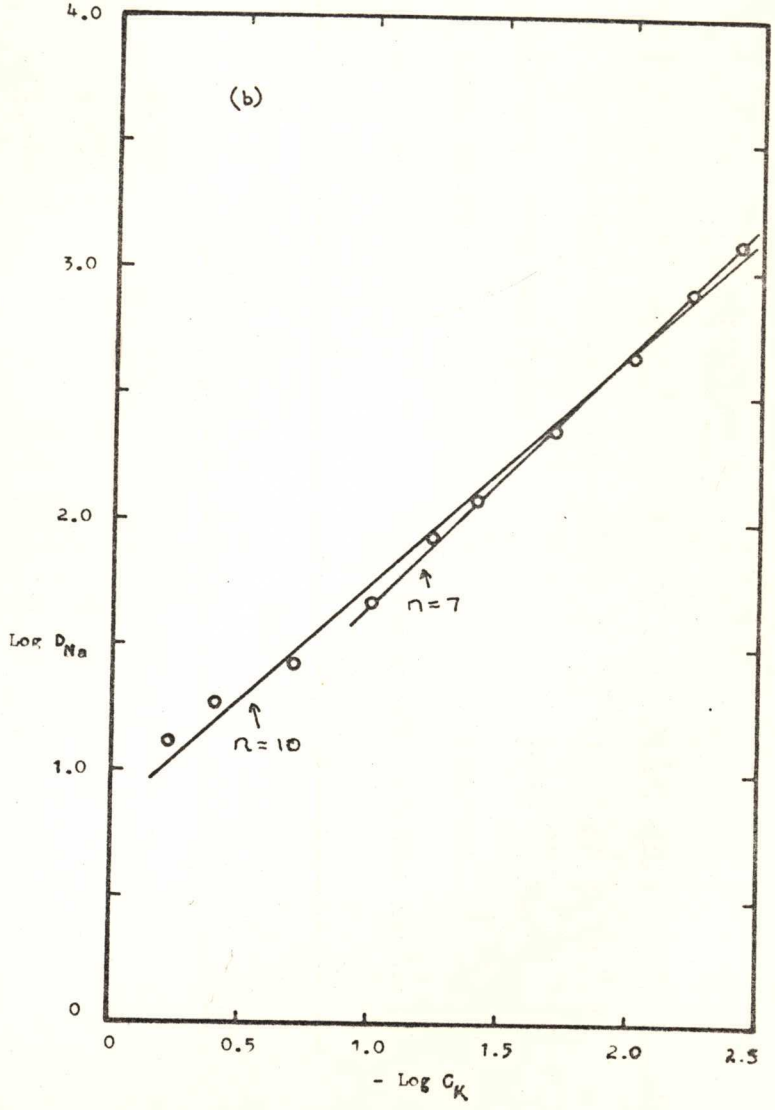
(b)
4.0
3.0
2.0
1.0
0
Log D_{Na}
n=10
n=7
0
0.5
1.0
1.5
2.0
2.5
- Log C_K

APPENDIX 12

Distribution of sulphate ion as a function of iodide concentration

Iodide ion concentration range:- 5.81×10^{-1} to 1.95×10^{-2} M.

Sulphate ion concentration:- $\sim 10^{-10}$ M.

pH of test solutions:- neutral.

Anion-exchange resin:- Dowex 1X8, 50-100 mesh.

$-\log C_I$	$\log D_S$
2.391	2.49 ± 0.04
2.236	2.12 ± 0.05
2.115	1.98 ± 0.06
2.017	1.78 ± 0.06
1.710	1.07 ± 0.09
1.391	0.53 ± 0.05
1.236	0.12 ± 0.02

FIGURE 12

(compiled from Appendix 12)

Measurement of the charge on the iodide ion

Slope of line (least squares analysis) = 2.02 ± 0.05

Apparent charge = -0.99 ± 0.02

Correlation coefficient = 1.00

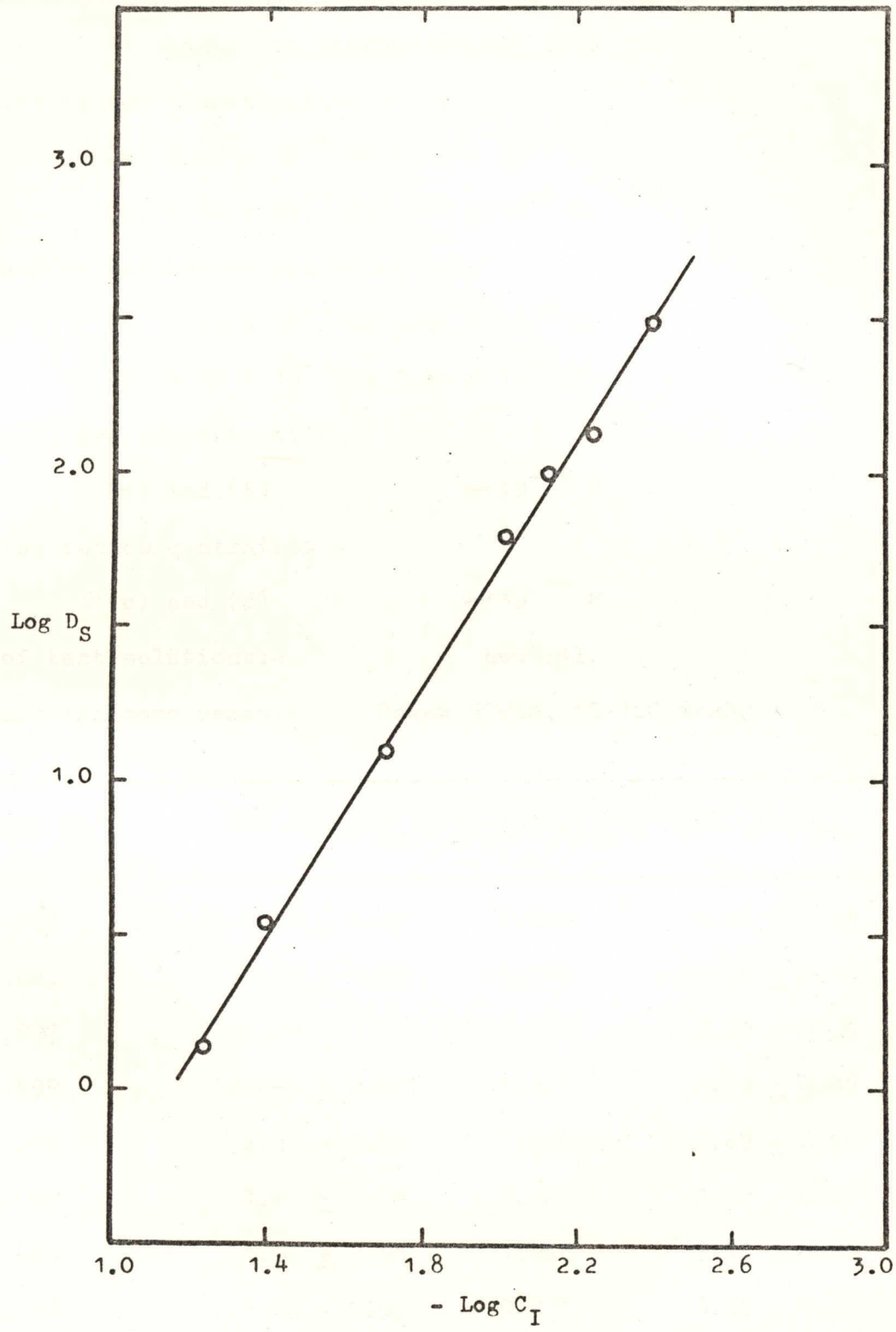
3.0
2.0
1.0
0
Log D_S
1.0
1.4
1.8
2.2
2.6
3.0
- Log C_I

APPENDIX 13

Caesium and cerium microcomponent ions with potassium and magnesium macrocomponent ions

Potassium ion concentration range:-

(a) 4.00×10^{-1} to 4.00×10^{-3} M.

(c) 3.60×10^{-1} to 2.40×10^{-3} M.

Magnesium ion concentration range:-

(b) 3.49×10^{-1} to 3.49×10^{-3} M.

(d) 4.19×10^{-1} to 2.53×10^{-3} M.

Caesium ion concentration:-

(a) and (b) $\sim 10^{-10}$ M.

Cerium ion concentration:-

(c) and (d) $\sim 10^{-10}$ M.

pH of test solutions:- neutral.

Cation-exchange resin:- Dowex 50WX8, 50-100 mesh.

$-\log C_K$	(a) $\log D_{Cs}$	$-\log C_K$	(c) $\log D_{Ce}$
2.398	3.11 ± 0.03	2.620	4.22 ± 0.03
2.222	2.93 ± 0.02	2.319	4.09 ± 0.03
2.097	2.79 ± 0.02	2.088	3.89 ± 0.05
1.699	2.443 ± 0.005	1.921	3.83 ± 0.09
1.398	2.18 ± 0.02	1.620	3.69 ± 0.05
1.097	1.97 ± 0.04	1.222	3.66 ± 0.05
0.824	1.57 ± 0.01	1.046	3.45 ± 0.06
0.398	1.05 ± 0.03	0.921	3.25 ± 0.03
		0.444	3.06 ± 0.03

$-\log C_{Mg}$	(b) $\log D_{Cs}$	$-\log C_{Mg}$	(d) $\log D_{Ce}$
2.457	2.239 ± 0.009	2.598	3.94 ± 0.09
1.980	1.96 ± 0.01	2.519	4.17 ± 0.07
1.774	1.845 ± 0.002	2.457	3.86 ± 0.08
1.281	1.579 ± 0.007	2.378	4.00 ± 0.05
1.075	1.459 ± 0.005	2.230	3.88 ± 0.06
0.758	1.285 ± 0.006	2.150	3.72 ± 0.08
		2.075	3.89 ± 0.06
		1.996	3.73 ± 0.05
		1.980	3.82 ± 0.02
		1.901	3.68 ± 0.04
		1.774	3.67 ± 0.05
		1.694	3.70 ± 0.05
		1.457	3.54 ± 0.03
		1.378	3.44 ± 0.03
		1.281	3.39 ± 0.02
		1.202	3.22 ± 0.03
		1.075	3.11 ± 0.03
		0.996	3.12 ± 0.05
		0.804	2.78 ± 0.04
		0.758	2.73 ± 0.04
		0.600	2.54 ± 0.02
		0.554	2.39 ± 0.03
		0.457	2.28 ± 0.01
		0.378	2.19 ± 0.04

FIGURE 13

(compiled from Appendix 13)

The effect of varying the microcomponent

	slope of line (least squares fit)	apparent charge	correlation coefficient
(a)	0.99 ± 0.06	+ 1.01 ± 0.06	1.00
(b)	0.55 ± 0.02	+ 1.82 ± 0.07	1.00
(c)	0.52 ± 0.07	+ 5.8 ± 0.8	0.98
(d)(n=24)	0.8 ± 0.2	+ 3.8 ± 0.8	0.96
(n=12)	1.27 ± 0.05	+ 2.36 ± 0.09	0.99

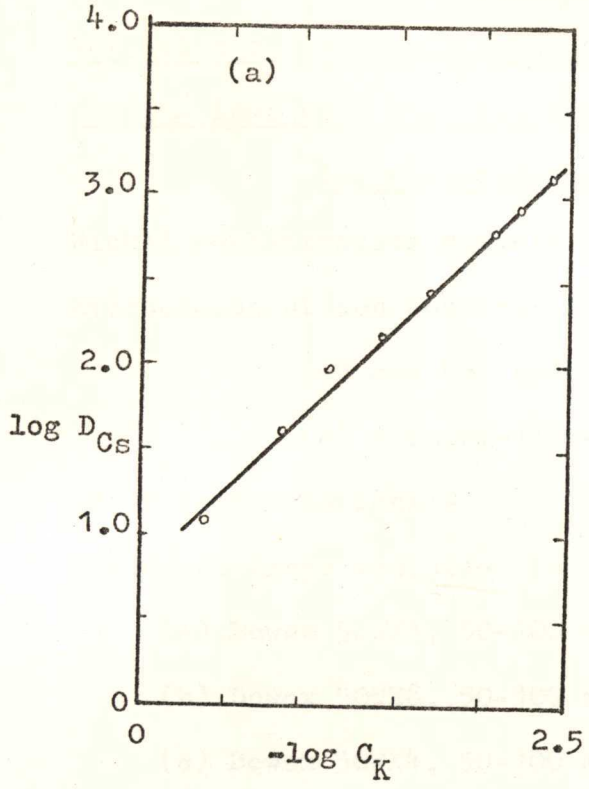
(a)
4.0
3.0
2.0
1.0
0
log D_{Cs}
0
2.5
-log C_K

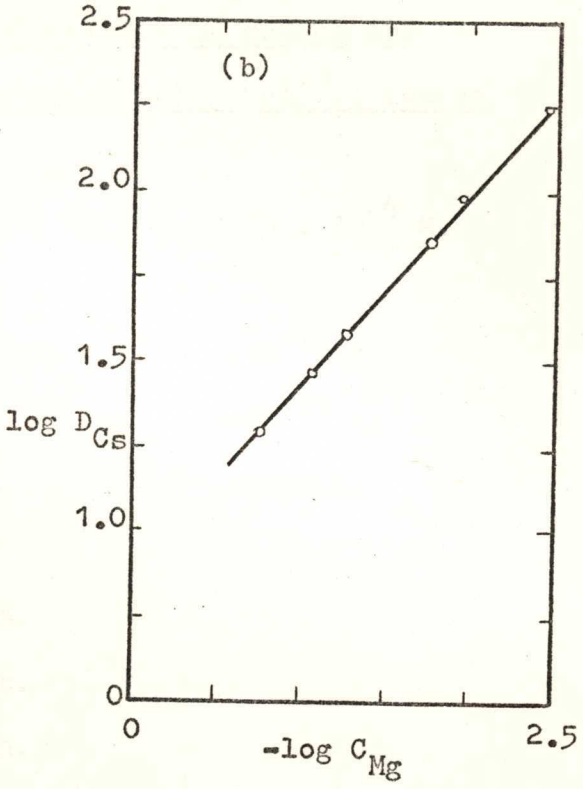
(b)
2.5
2.0
1.5
1.0
0
log D_{Cs}
0
2.5
-log C_{Mg}

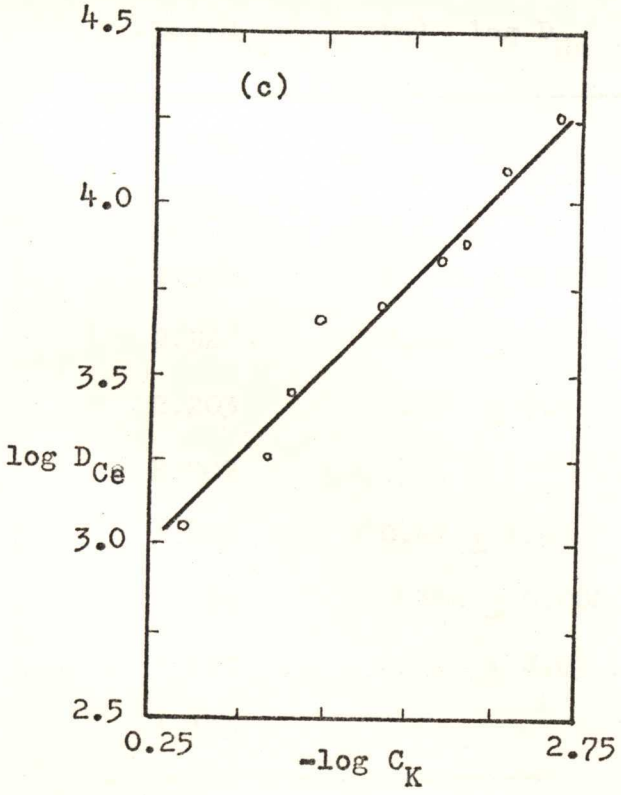
(c)
4.5
4.0
3.5
3.0
2.5
log D_{Ce}
0.25
2.75
-log C_K

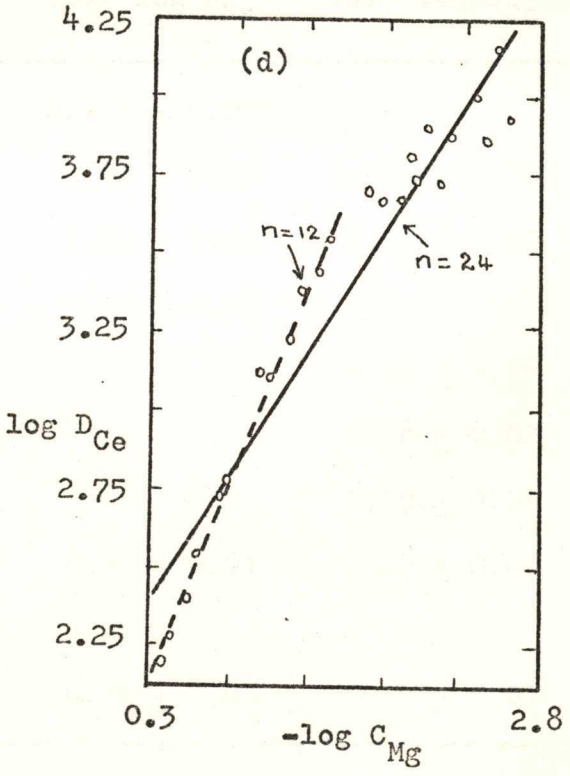
(d)
4.25
3.75
3.25
2.75
2.25
log D_{Ce}
n=12
n=24
0.3
2.8
-log C_{Mg}

APPENDIX 14

Variation of the distribution coefficients of sodium and caesium ions with the tris(ethylenediamine)nickel(II) ion as the macrocomponent ion

Nickel concentration range:- 7.83×10^{-2} to 7.83×10^{-4} M.

Microcomponent ion concentration :-

(a) and (b) sodium-22:- $\sim 10^{-10}$ M.

(c) caesium-137:- $\sim 10^{-10}$ M.

pH of test solutions:- neutral.

Cation-exchange resins:-

(a) Dowex 50WX4, 50-100 mesh.

(b) Dowex 50WX8, 50-100 mesh.

(c) Dowex 50WX4, 50-100 mesh.

$-\log C_{Ni}$	(a) $\log D_{Na}$	(b) $\log D_{Na}$	(c) $\log D_{Cs}$
3.106		0.910 ± 0.005	
2.805		0.87 ± 0.02	1.009 ± 0.006
2.504	0.723 ± 0.009	0.80 ± 0.02	0.55 ± 0.02
2.328	0.663 ± 0.007	0.57 ± 0.06	
2.203	0.56 ± 0.02		0.53 ± 0.06
2.027			0.38 ± 0.02
1.805	0.42 ± 0.03		0.29 ± 0.02
1.629	0.300 ± 0.002	0.45 ± 0.01	0.27 ± 0.03
1.407	0.12 ± 0.02		
1.106		0.24 ± 0.03	0.14 ± 0.01

FIGURE 14

(compiled from Appendix 14)

Measurement of the charge of a complex ion

The tris(ethylenediamine)nickel(II) ion

	slope of line (least squares fit)	apparent charge	correlation coefficient
(a)	0.48 ± 0.02	+ 2.08 ± 0.08	1.00
(b)	0.3 ± 0.1	+ 3.3 ± 0.9	0.98
(c)	0.5 ± 0.1	+ 2.0 ± 0.4	0.91

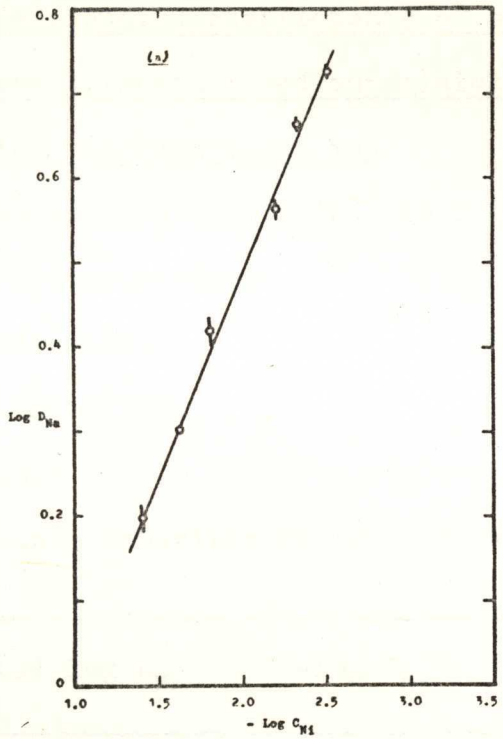
(a)
0.8
0.6
0.4
0.2
0
Log D_{Na}
1.0
1.5
2.0
2.5
3.0
3.5
- Log C_{Ni}

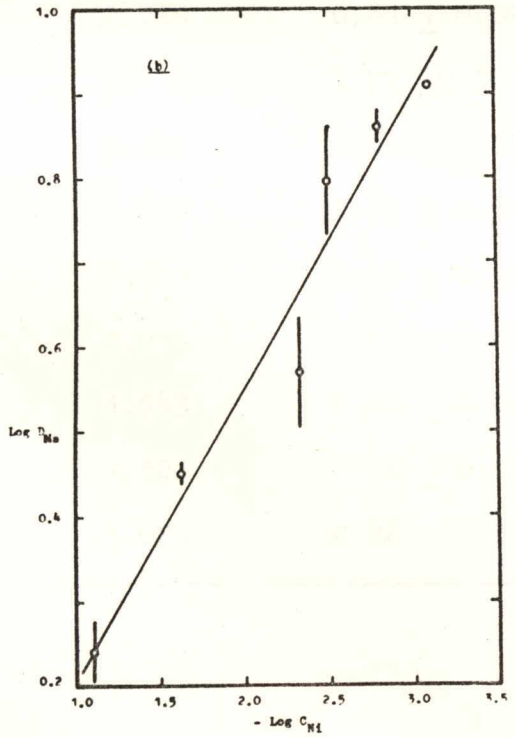
(b)
1.0
0.8
0.6
0.4
0.2
Log D_{Na}
1.0
1.5
2.0
2.5
3.0
- Log C_{Ni}

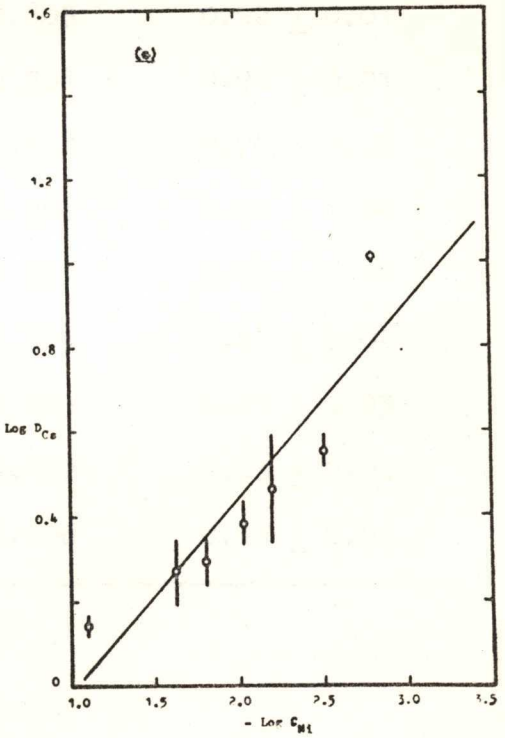
(c)
1.6
1.2
0.8
0.4
0
Log D_{Cs}
1.0
1.5
2.0
2.5
3.0
- Log C_{Ni}

APPENDIX 15

Variation of the distribution coefficients of sodium and caesium ions with the tris(ethylenediamine)nickel(II) ion as the macrocomponent ion

Nickel concentration range:- 9.54×10^{-2} to 7.83×10^{-4} M.

Microcomponent ion concentration:-

(a) sodium-22, $\sim 10^{-10}$ M.

(b) caesium-137, $\sim 10^{-10}$ M.

pH of test solutions:- neutral.

Cation-exchange resin:- Amberlite CG 120, 8% DVB, 100-200 mesh.

$-\log C_{Ni}$	(a) $\log D_{Na}$	$-\log C_{Ni}$	(b) $\log D_{Cs}$
3.021	0.85 ± 0.02	3.106	1.05 ± 0.02
2.719	0.81 ± 0.02	2.805	0.92 ± 0.01
2.418	0.77 ±0.02	2.504	0.91 ± 0.01
2.242	0.64 ± 0.03	2.328	0.74 ± 0.03
2.117	0.67 ± 0.01	2.203	0.72 ± 0.01
1.941	0.45 ± 0.02	2.027	0.78 ± 0.02
1.719	0.44 ± 0.02	1.805	0.64 ± 0.02
1.543	0.45 ± 0.02	1.629	0.61 ± 0.03
1.321	0.36 ± 0.03	1.407	0.53 ± 0.02
1.021	0.28 ± 0.02	1.106	0.47 ± 0.01

FIGURE 15

(compiled from Appendix 15)

Measurement of the charge of a complex ion

The tris(ethylenediamine)nickel(II) ion

	slope of line (least squares fit)	apparent charge	correlation coefficient
(a)	0.31 ± 0.05	+ 3.2 ± 0.5	0.95
(b)	0.29 ± 0.04	+ 3.5 ± 0.5	0.98

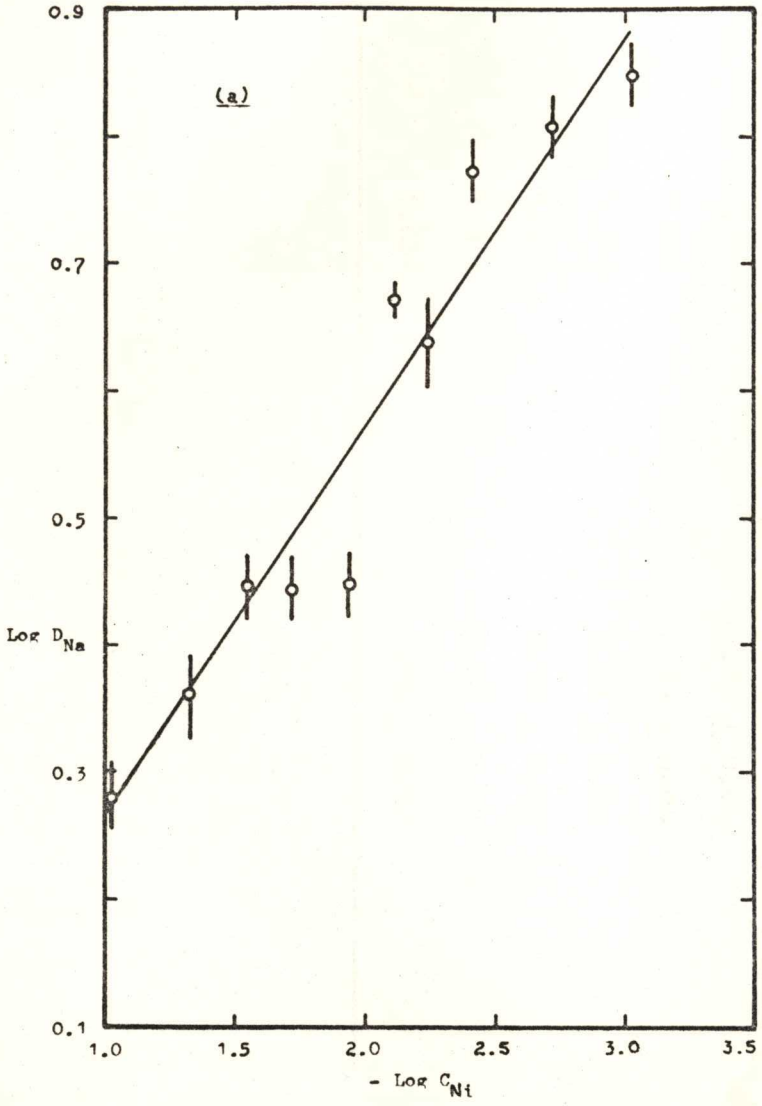
(a)
0.9
0.7
0.5
0.3
0.1
Log D_{Na}
1.0
1.5
2.0
2.5
3.0
3.5
- Log C_{Ni}

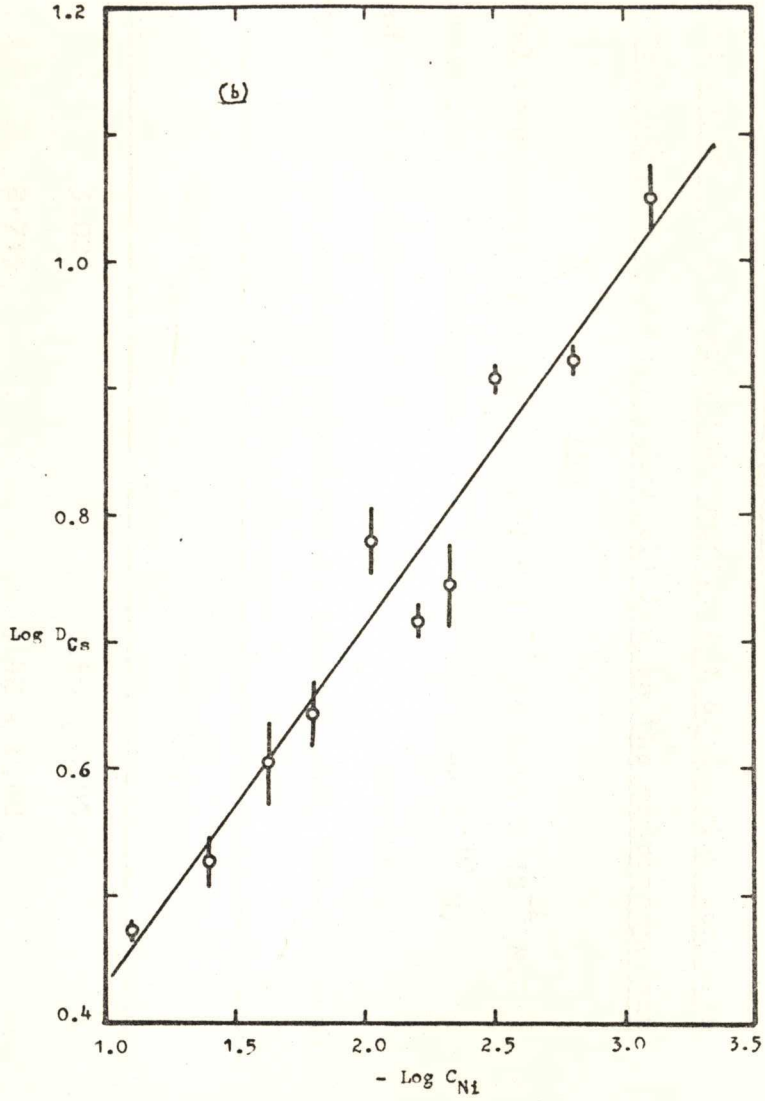
(b)
1.2
1.0
0.8
0.6
0.4
Log D_{Cs}
1.0
1.5
2.0
2.5
3.0
3.5
- Log C_{Ni}

APPENDIX 16

Variation of the distribution coefficient of calcium ion with the tris(ethylenediamine)nickel(II) ion as the macrocomponent ion

Nickel concentration range:- 9.54×10^{-2} to 9.54×10^{-4} M.

Calcium ion concentration:- $\sim 10^{-10}$ M.

pH of test solutions:- neutral.

Cation-exchange resin:- Amberlite CG 120, 8% DVB, 100-200 mesh.

$-\log C_{Ni}$	$\log D_{Ca}$
3.021	3.56 ± 0.05
2·719	3.42 ± 0.02
2.418	3.17 ± 0.02
2.242	3.01 ± 0.02
2.117	2.79 ± 0.06
1.941	2.57 ± 0·04
1.719	2.41 ± 0.02
1.543	2.18 ± 0.02
1.321	2.04 ± 0.03
1.021	1.79 ± 0.02

FIGURE 16

(compiled from Appendix 16)

Measurement of the charge of a complex ion

The tris(ethylenediamine)nickel(II) ion

Slope of line (least squares analysis) = 1.00 ± 0.05

Apparent charge = + 2.0 ± 0.1

Correlation coefficient = 1.00

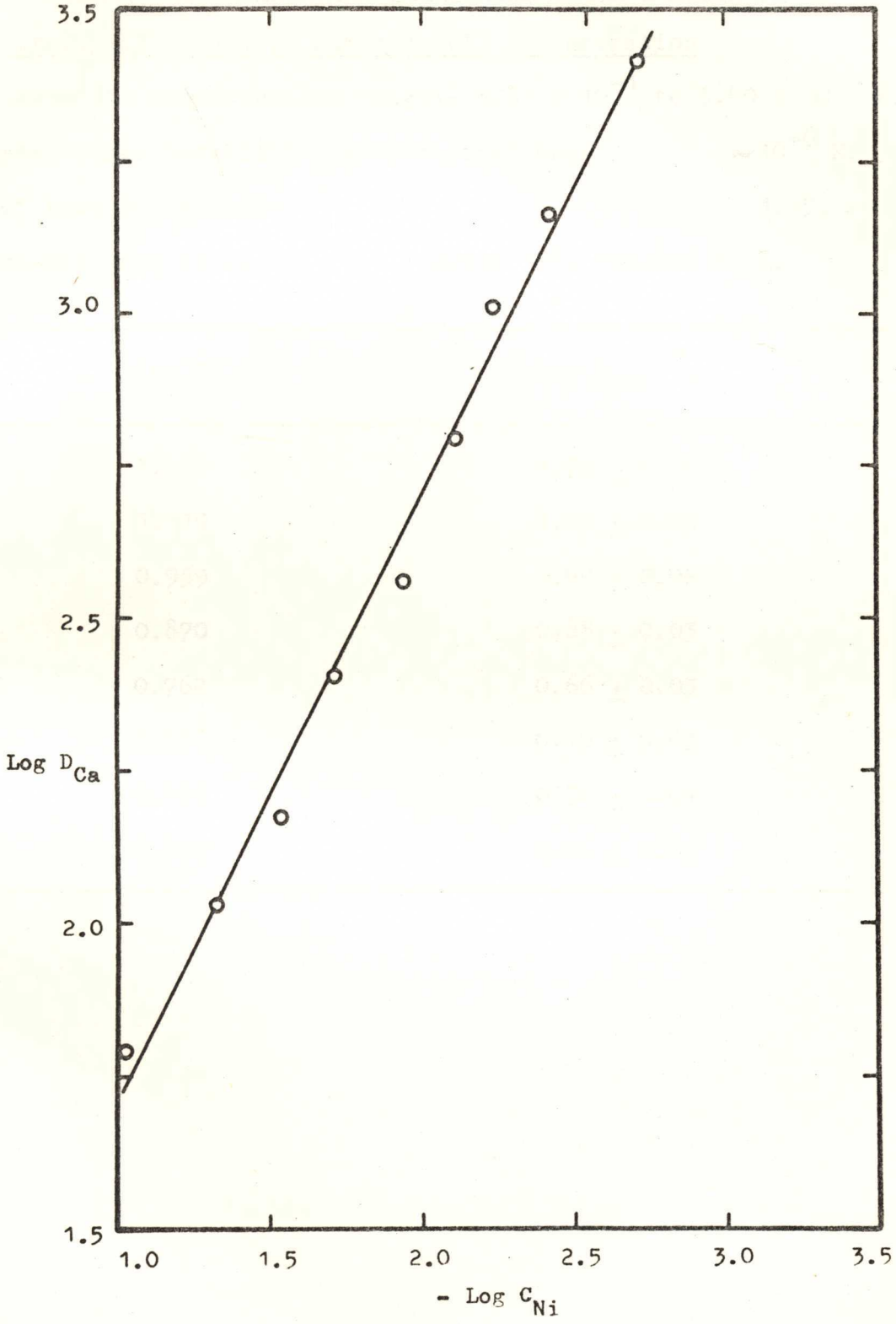
3.5
3.0
2.5
2.0
1.5
Log D_{Ca}
1.0
1.5
2.0
2.5
3.0
3.5
- Log C_{Ni}

APPENDIX 17

Variation of the distribution coefficient of the hexacyanocobaltate(III) ion with chromium(VI) concentration

Chromium(VI) concentration range:- 3.81×10^{-1} to 3.40×10^{-2} M.

Hexacyanocobaltate(III) ion concentration:- $\sim 10^{-6}$ M.

pH of test solutions:- 1.55.

Anion-exchange resin:- Dowex 1X8, 100-200 mesh.

$-\log C_{Cr}$	$\log D_{Co}$
1.469	1.75 ± 0.06
1.119	1.22 ± 0.02
0.959	0.99 ± 0.02
0.870	0.88 ± 0.03
0.762	0.66 ± 0.03
0.686	0.49 ± 0.03
0.599	0.36 ± 0.04
0.420	0.26 ± 0.03

FIGURE 17

(compiled from Appendix 17)

Measurement of the charge of a polymeric anion

The dichromate ion

Slope of line (least squares analysis) = 1.50 ± 0.05

Apparent charge = -2.00 ± 0.07

Correlation coefficient = 0.99

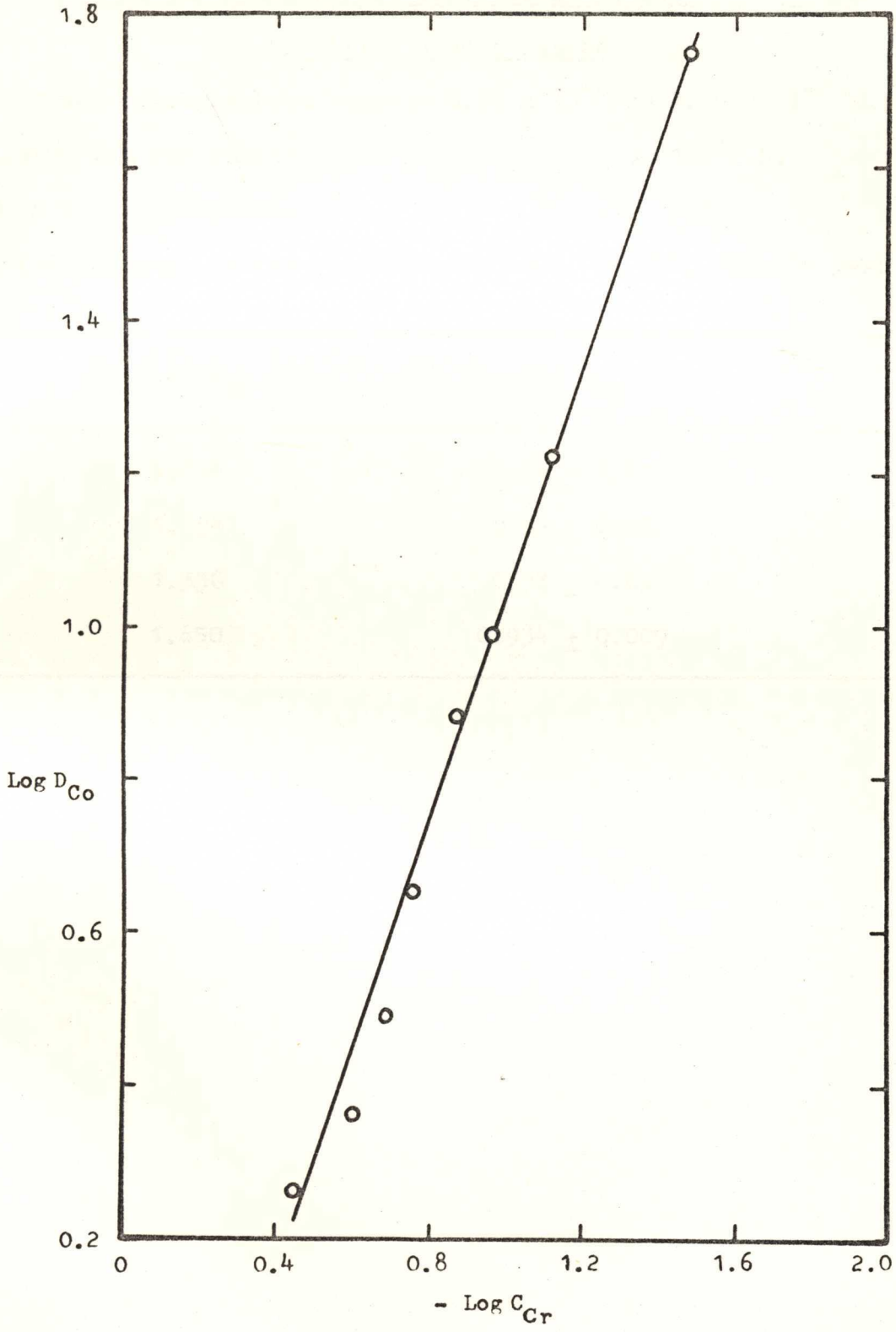
1.8
1.4
1.0
0.6
0.2
Log D_{Co}
0
0.4
0.8
1.2
1.6
2.0
- Log C_{Cr}

APPENDIX 18

Variation of the distribution coefficient of calcium-45 with beryllium concentration

Beryllium concentration range:- 8.02×10^{-2} to 2.24×10^{-2} M.

Calcium ion concentration:- $\sim 10^{-10}$ M.

pH of test solutions:- 5.50.

Cation-exchange resin:- Amberlite CG 120, 8% DVB, 100-200 mesh.

$-\log C_{Be}$	$\log D_{Ca}$
1.096	0.58 ± 0.01
1.194	0.62 ± 0.02
1.336	0.73 ± 0.03
1.650	0.934 ± 0.009

FIGURE 18

(compiled from Appendix 18)

The charge of the polymeric beryllium ion

Slope of line(least squares analysis) = 0.66 ± 0.01

Apparent charge = + 3.03 ± 0.04

Correlation coefficient = 1.00

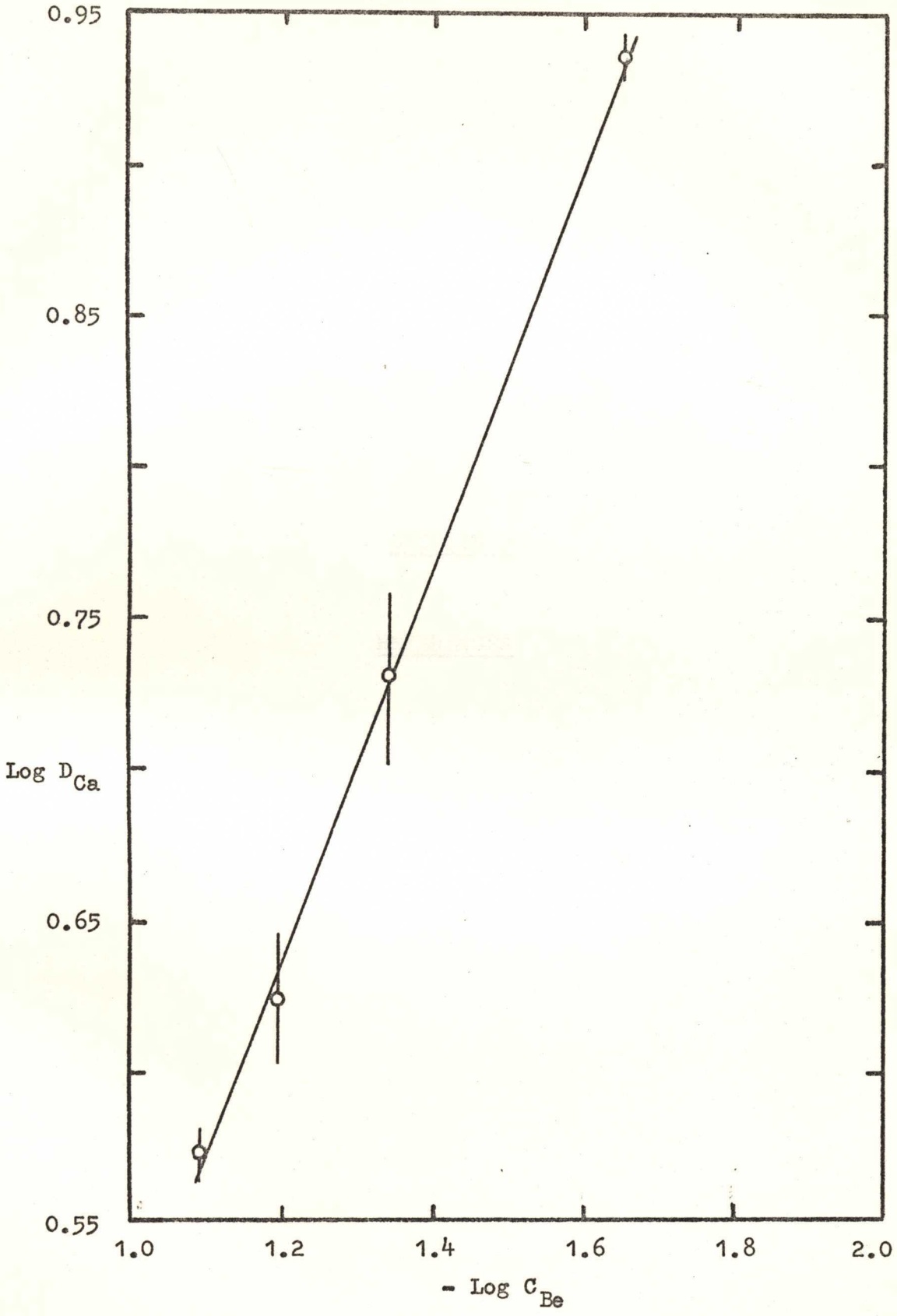
0.95
0.85
0.75
0.65
0.55
Log D_{Ca}
1.0
1.2
1.4
1.6
1.8
2.0
- Log C_{Be}

SECTION 7

REFERENCES

1. Strickland, J.D.H., Nature, 169, 620, (1952).

2. Welch, G.A., Nature, 172, 458, (1953).

3. Cady, H.H. and Connick, R.E., J. Amer. Chem. Soc., 80, 2646, (1958).

4. Jakovac, Z., and Lederer, M., J. Chromatog., 2, 413, (1959).

5. Nabivanets, B.I., Zhur. Neorg. Khim., 7, 412, (1962).
(Russ. J. Inorg. Chem., 7, 212, (1962).)

6. Curley, T.G.P., B.Sc. (Hons) Thesis, University of Sydney, (1964).

7. Kakihana, H. and Sillen, L.G., Acta Chem. Scand., 10, 985, (1956).

8. Smith, F.W., J. Inorg. Nucl. Chem., 29, 1161, (1967).

9. Cooper, M.K. and Foster, D.M., J. Chem. Soc., (A), 2968, (1968).

10. (a) Stepanova, L.N. and Trofimov, A.M., Radiokhimiya, 1, 403, (1959).

(b) Stepanova, L.N. and Trofimov, A.M., Zhur. Fiz. Khim., 34, 1837, (1960).
(Russ. J. Phys. Chem., 34, 874, (1960).)

(c) Stepanova, L.N. and Trofimov, A.M., Svensk Kem. Tidskr. 73, 72, (1961).

11. Grinberg, A.A., Stepanova, L.N. and Trofomov, A.M., Radiokhimiya, 2, 78, (1960).
(Radiochemistry, 2, 22, (1961).)

12. Grinberg, A.A., Petrzhak, G.I. and Stepanova, L.N., Radiokhimiya, 10, 96, (1968).
(Soviet Radiochemistry, 10, 90, (1968).)

13. Karago, L.V., Petrzhak, G.I. and Stepanova, L.N., Radiokhimiya, 12, 266, (1970). (Soviet Radiochemistry, 12, 240, (1970).)

14. Wallace, R.M., J. Phys. Chem., 68, 2418, (1964).

15. Mayer, S.W. and Tompkins, E.R., J. Amer. Chem. Soc., 69, 2866, (1947).

16. Garman, D.E.J., M.Sc. Thesis, University of Sydney, (1969).

17. Kraus, K.A. and Nelson, F., "The Structure of Electrolyte Solutions", W.J.Hammer (Ed), John Wiley, New York, pp.340 et seq, (1959).

18. Gregoire, C. and Paris, M.R., Anal. Chim. Acta, 42, 431, (1968).

19. Kakihana, H. and Maeda, M., Bull. Chem. Soc. Japan, 42, 1458, (1969).

20. idem, 43, 109, (1970).

21. Carpeni, G. and Lanza, E., Electrochim. Acta, 13, 519, (1968).

22. Lanza, E., Rev. Chem. Miner., 6, 653, (1969).

23. Helfferich, F., "Ion-Exchange", McGraw-Hill, New York, (1962). (a) 156, (b) 127, (c) 217, (d) 136, (e) 103, (f)230, (g) 283, (h) 118.

24. Whitney, D.C. and Diamond, R.M., Inorg. Chem., 2, 1284, (1963).

25. (a) Donnan, F.G., Z. Electrochem., 17, 572, (1911).
(b) Donnan, F.G., Z. Physik. Chem., A168, 369, (1934).

26. Donnan, F.G. and Guggenheim, E.A., Z. Physik. Chem., A162, 346, (1932).

27. Mayer, S.W. and Tompkins, E.R., J.Amer. Chem. Soc., 69, 2859, (1947).

28. Ferguson, J.A., B.Sc.(Hons) Thesis, University of Sydney, (1965).

29. Foster, D.M., B.Sc.(Hons) Thesis, University of Sydney, (1966).

30. Vogel, A.I.,"Quantitative Inorganic Analysis", Longmans, London, 3rd Edition, (1964).
(a) 434, (b)1161, (c) 267, (d) 259, (e) 242.

31. Palkans, P., "The Spectrophotometric Determination of Beryllium with Chrome Azurol S", AAEC Report, Jan., (1963).

32. State, H.M., "Inorganic Synthesis", Rochow, E.G. (Ed), McGraw-Hill, London, 6, 200, (1960).

33. Elwell, W.T., and Gidley, J.A.F., "Atomic Absorption Spectroscopy", Pergamon, London, 2nd Edition, p.109, (1966).

34. (a) Newton-Hayes, F., "Solutes and Solvents for Liquid Scintillation Counting", Packard Technical Bulletin Number 1, Packard Instrument Co., Illinois.

(b) Horrocks, D.L., "Liquid Scintillation Counting of Inorganic Radionucleotides", Packard Technical Bulletin Number 2, Packard Instrument Co., Illinois.

(c) Rapkin, E., "Determination of Radioactivity in Aqueous Solution", Packard Technical Bulletin Number 6, Packard Instrument Co., Illinois.

(d) Turner, J.C., "Sample Preparation for Liquid Scintillation Counting", The Radiochemical Centre, Amersham, England, (1967).

35. Bent, H.A., Chem. Revs. 68, 587, (1968).

36. "Manual for pH Meter 4", Radiometer Ltd., Copenhagen.

37. "Provisional Operating Instructions for the Philips PW4305 Coincidence Unit", Philips Scientific and Analytical Equipment Department", Eindoven, The Netherlands.

38. Lambie, D.A., "Techniques for the Use of Radioisotopes in Analysis", Spon, London, pp.115-7, (1964).

39. Diem, K., "Documenta Geigy Scientific Tables", Geigy Pharmaceuticals, pp.36-7, (1963).

40. Cooper, M. K., and Salmon, J.E., J. Chem. Soc., 2009, (1962).

41. Salmon, J.E. and Hale, K.D., "Ion-Exchange, a Laboratory Manual", Butterworths, London, (1959). (a) 86, (b) 85.

42. Kunin, R., and Myers, J., J. Amer. Chem. Soc., 69, 2874, (1947).

43. Connick, R.E. and Mayer, S.W., J. Amer. Chem. Soc., 73, 1176, (1951).

Choppin, G.R. and Unrein, P.J., J. Inorg. Nucl. Chem., 25, 387, (1963).

44. Brescia, F., Arents, J., Meislich, H. and Turk, A., "Fundamentals of Chemistry, a Modern Introduction", Academic, New York, p. 176, (1970).

45. Dehn, W.M., J. Amer. Chem. Soc., 36, 829, (1914).

Viterbi, E. and Krausz, G., Gazz. Chim. Ital., 57, 690, (1927).

Jander, G. and Spandau, H., Z. anorg. allgem. Chem., 249, 67, (1942).

46. Martens, A. and Carpeni, G., J.Chim. Phys., 60, 534, (1963).

47. Russel, R.U. and Salmon, J.E., J.Chem. Soc., 4708, (1958); 3211, (1961).

48. Schubert, J., Russel, E.R. and Myers, L.S., J. Biol. Chem., 185, 387, (1950).

49. Youden, W.J., "Statistical Methods for Chemists", John Wiley, New York, pp.41-2, (1957).

50. Daniels, F., Williams, J.W., Bender, P., Alberty, R.A. and Cornwell, C.D., "Experimental Physical Chemistry", McGraw-Hill, New York, 6th Edition, p.395, (1962).

Acknowledgements

I wish to thank Professors R.J.W.LeFevre and H.C.Freeman for allowing me to carry out this work in their department.

Sincere thanks are due to my supervisor, Dr M.K.Cooper, for the constant help and encouragement that he has given to me during the past two years.

Furthermore I would like to express my gratitude to other members of the Chemistry School, especially Mr D.E.J.Garman, for their friendship and help during the course of this work.

The thesis was typed by my sister, Mrs G.McPhee, to whom I am deeply indebted.

Finally, I wish to thank the Australian Atomic Energy Commission for the use of the Philips radioactive counting equipment.

Darryl Yaniuk
23 March, 1972.